

The Pennsylvania State University  
The Graduate School  
Department of Civil and Environmental Engineering

**In-line Treatment of Metal Contaminated Storm Water by  
Charred Microporous Polymers.**

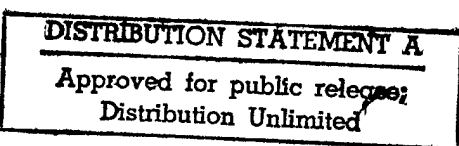
A Thesis in  
Environmental Engineering  
by  
John Anthony Kliem

© 1998 John Anthony Kliem

Submitted in Partial Fulfillment  
of the Requirements  
for the Degree of

Master of Science

August 1998



I grant The Pennsylvania State University the nonexclusive right to use this work for the University's own purposes and to make single copies of the work available to the public on a not-for-profit basis if copies are not otherwise available.

  
John Anthony Klein

We approve the thesis of John Anthony Kliem.

Date of Signature

William D. Burgos

William D. Burgos  
Assistant Professor of Environmental Engineering  
Thesis Advisor

6/17/98

Brian A. Dempsey

Brian A. Dempsey  
Associate Professor of Environmental Engineering.

6/12/98

Raymond W. Regan, Sr.

Raymond W. Regan, Sr.  
Professor of Environmental Engineering

6/12/98

Paul P. Jovanis

Paul P. Jovanis  
Professor of Civil Engineering  
Head of Department of Environmental and Civil  
Engineering

6/12/98

## ABSTRACT

This paper examines the feasibility of using an in-line storm water treatment system to remove heavy metals from storm water discharges. There are a number of commercially available microporous carbons that have a demonstrated affinity for the uptake of metals. Industry currently utilizes in-line storm water treatment processes to remove settle able solids, oils and greases; these processes could easily be altered to include the adsorption of dissolved contaminants such as metals. Two charred microporous polymers, Supelcarb<sup>TM</sup> and Carboxen-1011<sup>TM</sup> were measured for adsorption capacity for Cu<sup>2+</sup> and Ni<sup>2+</sup> removal in both batch and flow through experiments. Results indicate Cu<sup>2+</sup> was removed but not Ni<sup>2+</sup>.

A scenario was conducted based on experimentally derived Cu<sup>2+</sup> adsorption results to estimate the filter service time for the adsorbers tested when placed with in existing in-line storm water treatment system and exposed to Cu<sup>2+</sup> contaminated storm water. Storm water flows from 1, 2, 5, and 10 years storms were evaluated. Filter service time for the 1 year storm was 3.5 and 6 hours for Supelcarb<sup>TM</sup> and Carboxen-1011<sup>TM</sup> respectively. As storm intensity increased the filter service time decreased. This scenario illustrates that Supelcarb<sup>TM</sup> and Carboxen-1011<sup>TM</sup> are not good adsorbers in this situation. However, removal of heavy metal contaminated storm water by charred microporous polymer adsorption is a viable pollution control strategy.

## TABLE OF CONTENTS

|  |     |
|--|-----|
| LIST OF FIGURES.....   | vii |
| LIST OF TABLES .....   | x   |
| ACKNOWLEDGMENTS.....   | xi  |
| Chapter 1 INTRODUCTION .....   | 1   |
| Chapter 2 BACKGROUND .....   | 4   |
| 2.1 CARBON ADSORBENTS.....   | 4   |
| 2.1.1 Naturally Occurring Activated Carbons .....                      | 5   |
| 2.1.1.1 Peat .....   | 5   |
| 2.1.1.2 Bone Char .....  | 7   |
| 2.1.2 Polymer Carbons.....   | 7   |
| 2.1.2.1 SupelCarb™ .....   | 8   |
| 2.1.2.2 Carboxen – 1011™ .....   | 10  |
| 2.1.3 Mesoporous Silica Materials with Functionalized Monolayers ..... | 10  |
| 2.2 Adsorption Mechanisms .....  | 11  |
| 2.2.1 van der Waals Force .....  | 11  |
| 2.2.2 Adsorption From Solution .....                                   | 13  |
| 2.2.3 Pore Diffusion.....  | 14  |
| 2.2.4 Quiescent Liquid – Solid Adsorption .....                        | 14  |
| 2.2.5 Fixed Bed Adsorption .....                                       | 15  |
| 2.3 Metal Adsorption .....   | 15  |
| 2.4 Storm Water Best Management Practices .....                        | 17  |
| 2.4.1 Oil/Water Separators.....  | 18  |
| 2.4.2 Storm Water Settling Basins.....                                 | 18  |
| 2.4.3 Peat Sand Filter.....  | 19  |
| Chapter 3 METHODS AND MATERIALS .....                                  | 24  |
| 3.1 Overview of the Test Program.....                                  | 24  |
| 3.2 Materials .....  | 25  |
| 3.2.1 Adsorbents .....   | 25  |
| 3.2.2 Synthetic Storm water Solutions.....                             | 25  |
| 3.2.2.1 Stock Solutions .....  | 27  |

|  |    |
|--|----|
| 3.2.2.1.1 Rinse and Dilution for the Influent Solutions:<br>100mM NaCl with pH Buffer.....   | 27 |
| 3.2.2.1.2 Dilution for Stock Solutions: 100 mM NaCl without<br>pH Buffer.....  | 27 |
| 3.2.2.1.3 Stock Solution: 5000 mg Cu <sup>2+</sup> /L.....   | 28 |
| 3.2.2.1.4 Stock Solution: 10 mg Cu <sup>2+</sup> /L.....   | 28 |
| 3.2.2.1.5 Stock Solution: 1000 mg Ni <sup>2+</sup> /L.....   | 28 |
| 3.2.2.1.6 Stock Solution: 10 mg Ni <sup>2+</sup> /L.....   | 29 |
| 3.2.2.2 Batch Experiment Solutions .....   | 29 |
| 3.2.2.3 Flow Through Experiment Solutions: .....   | 29 |
| 3.3 Experimental Methods.....  | 32 |
| 3.3.1 Batch Experiments .....  | 32 |
| 3.3.2 Flow Through Experiments .....   | 34 |
| 3.4 Analytical Methods.....  | 36 |
| 3.4.1 Atomic Absorption Spectrometry .....   | 36 |
| 3.4.2 AAS Calibration .....  | 37 |
| 3.4.2.1 Calibration Solutions for Cu <sup>2+</sup> .....   | 38 |
| 3.4.2.2 Calibration Solution: 1 mg Cu <sup>2+</sup> /L .....   | 38 |
| 3.4.2.3 Calibration Solution for Ni <sup>2+</sup> .....  | 38 |
| 3.4.2.4 Calibration Solution: 0.5 mg Ni <sup>2+</sup> /L .....   | 39 |
| 3.5 Data Reduction .....   | 40 |
| 3.5.1 Batch Data Handling.....   | 40 |
| 3.5.2 Flow Through Data Handling .....   | 42 |
| Chapter 4 RESULTS AND DISCUSSION.....  | 47 |
| 4.1 Results.....   | 47 |
| 4.1.1 Cu <sup>2+</sup> in Synthetic Storm Water .....  | 47 |
| 4.1.1.1 Batch Results for Cu <sup>2+</sup> .....   | 47 |
| 4.1.1.2 Flow Through Results for Cu <sup>2+</sup> .....  | 50 |
| 4.1.2 Ni <sup>2+</sup> in Synthetic Storm Water.....   | 51 |
| 4.1.2.1 Batch Results for Ni <sup>2+</sup> .....   | 51 |
| 4.1.2.2 Flow through Results for Ni <sup>2+</sup> .....  | 51 |
| 4.1.3 Competitive Adsorption Flow Through Results for Cu <sup>2+</sup> and Ni <sup>2+</sup> .....  | 53 |
| 4.2 Discussion.....  | 54 |
| 4.2.1 Cu <sup>2+</sup> Adsorbing on to Supelcarb <sup>TM</sup> and Carboxen-1011 <sup>TM</sup> in the<br>Batch Experiments.....              | 54 |
| 4.2.2 Ni <sup>2+</sup> Adsorbing on to Supelcarb and Carboxen .....  | 55 |
| 4.2.3 Minteq Chemical Speciation Model of Batch Tests .....  | 56 |
| 4.2.4 Feasibility Analysis on the Use of Microporous Treatment of<br>Metal Contaminated Storm Water by Charred Microporous<br>Polymers ..... | 58 |
| Chapter 5 CONCLUSIONS AND RECOMMENDATIONS .....  | 75 |

|                           |           |
|---------------------------|-----------|
| 5.1 Conclusions.....      | 75        |
| 5.2 Recommendations.....  | 76        |
| <b>BIBLIOGRAPHY .....</b> | <b>78</b> |

## LIST OF FIGURES

|   |    |
|---|----|
| <i>Figure 2-1:</i> Typical van der Waals force between a molecule and a planar surface as a function of separation diameter (Jenkins, 1976).....  | 20 |
| <i>Figure 2-2:</i> Adsorption column mass transfer zone (Snoeyink, 1990).....   | 21 |
| <i>Figure 2-3:</i> Stormceptor <sup>TM</sup> oil/water separator plan and profile view. Storm water enters the upper chamber and goes to the lower chamber. Grit is deposited in the lower chamber and oils and greases will accumulate in the top. During high storm water flows most of the water bypasses the lower chamber and exits the separator..... | 22 |
| <i>Figure 2-4:</i> Stormwater settling basin (Dunn et al., 1995). Extended drainage ponds are effective for treating drainage water from 10 acres. This design has been shown to remove 60 to 80% of suspended solids. .....  | 23 |
| <i>Figure 3-1:</i> Elevation view of a typical adsorbent column (Snoeyink, 1990). .....   | 44 |
| <i>Figure 3-2:</i> Schematic of experimental apparatus for the flow through tests. ....   | 44 |
| <i>Figure 3-3:</i> Single beam atomic absorption spectrometer (Fifield and Haines, 1995). .....   | 45 |
| <i>Figure 3-4:</i> Representative AAS calibration curve. ....   | 45 |
| <i>Figure 3-5:</i> Sample time to breakthrough curve showing triplicate sets of one experimental condition.....   | 46 |
| <i>Figure 4-1:</i> Copper adsorption isotherm obtained with Supelcarb <sup>TM</sup> in the batch experiments. ....  | 63 |
| <i>Figure 4-2:</i> Copper adsorption isotherm obtained with Carboxen-1011 <sup>TM</sup> in the batch experiments. ....  | 63 |
| <i>Figure 4-3:</i> Freundlich adsorption isotherm obtained with Supelcarb <sup>TM</sup> in the batch experiments. ....  | 64 |
| <i>Figure 4-4:</i> Copper breakthrough curves obtained with Supelcarb <sup>TM</sup> and a constant influent concentration of 5 mg Cu <sup>2+</sup> /L in the flow through   |    |

|   |    |
|---|----|
| experiments. Error bars represent a standard deviation about a triplicate mean.....   | 65 |
| <i>Figure 4-5: Copper breakthrough curves obtained with Supelcarb<sup>TM</sup> and a constant flow rate of 200 mL/min in the flow through experiments. Error bars represent a standard deviation about a triplicate mean (10 mg/L error bar no larger than symbol size). .....</i>            | 65 |
| <i>Figure 4-6: Copper breakthrough curves obtained with Carboxen-1011<sup>TM</sup> and a constant influent concentration of 5 mg Cu<sup>2+</sup>/L in the flow through experiments. Error bars represent a standard deviation about a triplicate mean.....</i>                                | 66 |
| <i>Figure 4-7: Copper breakthrough curves obtained with Carboxen-1011<sup>TM</sup> and a constant flow rate of 200 mL/min in the flow through experiments. Error bars represent a standard deviation about a triplicate mean (10 mg/L error bar no larger than symbol size). .....</i>        | 66 |
| <i>Figure 4-8: Nickel adsorption isotherm obtained with Supelcarb<sup>TM</sup> in the batch experiments.....</i>  | 67 |
| <i>Figure 4-9: Nickel adsorption isotherm obtained with Carboxen-1011<sup>TM</sup> in the batch experiments. .....</i>  | 67 |
| <i>Figure 4-10: Nickel breakthrough curves obtained with Supelcarb<sup>TM</sup> and a constant flow rate of 200 mL/min in the flow through experiments. Error bars represent a standard deviation about a triplicate mean.....</i>  | 68 |
| <i>Figure 4-11: Nickel breakthrough curves obtained with Carboxen-1011<sup>TM</sup> and a constant flow rate of 200 mL/min in the flow through experiments. Error bars represent a standard deviation about a triplicate mean.....</i>  | 68 |
| <i>Figure 4-12: Copper breakthrough in a Cu<sup>2+</sup>/Ni<sup>2+</sup> bisolute system. Curves obtained with Supelcarb<sup>TM</sup> and a constant flow rate of 300 mL/min in the flow through experiments. Error bars represent a standard deviation about a triplicate mean.....</i>      | 69 |
| <i>Figure 4-13: Copper breakthrough in a Cu<sup>2+</sup>/Ni<sup>2+</sup> bisolute system. Curves obtained with Carboxen-1011<sup>TM</sup> and a constant flow rate of 300 mL/min in the flow through experiments. Error bars represent a standard deviation about a triplicate mean. ....</i> | 69 |
| <i>Figure 4-14: Copper adsorption isotherm obtained with Supelcarb<sup>TM</sup>. Minteq model results plotted as dark square. ....</i>  | 70 |

|  |    |
|--|----|
| <i>Figure 4-15: Copper adsorption isotherm obtained with Carboxen-1011<sup>TM</sup>.<br/>Minteq model results plotted as dark square.....</i>  | 70 |
| <i>Figure 4-16: Nickel adsorption isotherm obtained with Supelcarb<sup>TM</sup> in the batch<br/>experiments with Minteq model results.....</i>  | 71 |
| <i>Figure 4-17: Nickel adsorption isotherm obtained with Carboxen-1011<sup>TM</sup> in the<br/>batch experiments with Minteq model results. ....</i>   | 71 |
| <i>Figure 4-18: Minteq model of of a combined Ni<sup>2+</sup> and Cu<sup>2+</sup> batch adsorption<br/>experiment with Supelcarb<sup>TM</sup>. Minteq simply super imposed the adsorption<br/>isotherms for each metal. This result is caused by Minteq's assumption of<br/>infinite adsorption sites on the charred porous polymers. ....</i>       | 72 |
| <i>Figure 4-19: Minteq model of of a combined Ni<sup>2+</sup> and Cu<sup>2+</sup> batch adsorption<br/>experiment with Carboxen-1011<sup>TM</sup>. Minteq simply super-positioned the<br/>adsorption isotherms for each metal. This result is caused by Minteq's<br/>assumption of infinite adsorption sites on the charred porous polymers.....</i> | 73 |
| <i>Figure 4-19:Graph demonstrates the linear relationship between flow rate, influent Cu<sup>2+</sup><br/>and bed volumes to filter break through using SupelcarbTM. This analysis should be<br/>used for adsorber filter design.....</i>  | 74 |
| <i>Figure 4-20:Graph demonstrates the linear relationship between flow rate, influent Cu<sup>2+</sup><br/>and bed volumes to filter break through using Carboxen-1011<sup>TM</sup>. This analysis<br/>should be used for adsorber filter design .....</i>  | 74 |

**LIST OF TABLES**

|  |    |
|--|----|
| <i>Table 2-1:</i> Physical characteristics of Supelcarb <sup>TM</sup> and Carboxen-1011 <sup>TM</sup> .....  | 9  |
| <i>Table 3-1:</i> Physical characteristics of Supelcarb <sup>TM</sup> and Carboxen-1011 <sup>TM</sup> .....  | 26 |
| <i>Table 3-2:</i> Volume of stock solution for a desired influent concentration used in the batch experiments.....   | 30 |
| <i>Table 3-3:</i> Volume of stick solution for a desired influent concentration used in the flow through experiments. ....   | 31 |
| <i>Table 4-1:</i> Summary of Freundlich adsorption isotherm coefficients for Supelcarb <sup>TM</sup> and Carboxen-1011 <sup>TM</sup> from batch experiments with Cu <sup>2+</sup> in synthetic storm water. .... | 49 |
| <i>Table 4-2:</i> Summary of Freundlich adsorption isotherm coefficients for Suplecarb <sup>TM</sup> and Carboxen-1011 <sup>TM</sup> from batch experiments with Ni <sup>2+</sup> in synthetic storm water. .... | 52 |
| <i>Table 4-3:</i> Analysis of charred microporous polymers as an in-line storm water treatment system.. ....   | 61 |

## ACKNOWLEDGMENTS

I appreciate the work my thesis advisor, Dr. William Burgos put into this project. His guidance and encouragement through all stages of this research and in completion of my course work has been invaluable. Many thanks to Gordon Clark whose analytical skill, mechanical abilities and friendship made this project a success. I also thank Drs. Brian Dempsey and Raymond Regan who served as thesis committee members and provided helpful insight to improve this research project. Finally to my wife Diane her patience, understanding, and support were essential in the completion of my Master of Science.

## Chapter 1

### INTRODUCTION

Common industrial activities such as metal cutting welding, surface preparation and painting are potential sources of heavy metal pollution. When these activities are performed outdoors, e.g. ship building and bridge construction, even with the most sophisticated best management practices (BMP), some heavy metals are invariably transported into storm water systems.

In a nation wide study conducted by the United States Environmental Protection Agency, the average urban runoff contains 53 µg/L total copper, 353 µg/L total zinc (EPA, 1983). As a result of that study, storm water discharges are facing increasing regulatory compliance requirements, which include not only BMP's but also chemical monitoring programs (Ellwood and Burgos, 1998). Heavy metals such as copper, lead, zinc, and nickel may become problematic for certain industrial activities to maintain compliance with new storm water National Pollutant Discharge Elimination Permits (NPDES).

A potentially effective storm water pollution prevention strategy is to use porous heavy metal adsorbers within storm water systems. Surface modified mesoporous silicas are very efficient at removing heavy metals in batch experiments (Feng *et al.*, 1997). Specialty carbons such as bone char also have excellent selectivity for heavy metal

(Brown, 1992). Peat, typically less expensive and more abundant compared to the previous two adsorbents, is also an effective material for heavy metal removal.

Conceptually, a heavy metal adsorber would function as a "sponge" effectively removing these contaminants as storm water passes through the porous matrix. Selection of the proper adsorbent material would depend on the selectivity, capacity, kinetics of heavy metal uptake under typical high flow conditions, porosity of the matrix, and headloss characteristics. In addition to material selection, placement of the porous adsorber within the storm water system must be given careful consideration.

In-line storm water treatment systems are currently part of BMPs at several industrial sites. These systems primarily treat the storm water for removal of oils, greases, and suspended solids. Oils and greases are usually removed in an in-line oil water separator. This unit process works by skimming the oil and grease off the top of the storm water. Suspended solids can be removed by channeling the storm water into a settling pond. Both of these unit processes are designed to be bypassed during high flow conditions. The heavy metal adsorber could be placed inside the oil/water separator or at the discharge point of a storm water-settling basin.

The objectives of this research were to: (1) evaluate the potential use of commercially available adsorbents for the removal of heavy metals from storm water at industrial locations; and (2) determine the feasibility of placing a porous adsorbent within a storm water collection system as a BMP.

A literature review was conducted of urban storm water treatment methods to investigate the possibility of incorporating adsorbents within storm water treatment

systems. The capacity and breakthrough characteristics of two commercially available adsorbents were evaluated. The adsorbents evaluated were Supelcarb<sup>TM</sup>, (Supelco<sup>TM</sup>, Bellefonte, PA), a charred microporous polymer with "dead end" pores; Carboxen-1011<sup>TM</sup> (Supelco<sup>TM</sup>, Bellefonte, PA) a charred microporous polymer with "throughput" pores. Batch adsorption experiments were conducted to determine the adsorption capacity of the two materials. The aquatic chemistry of the batch test results were modeled with Minteq (Allison et al., 1990) to analyze the metal speciation. The charred microporous polymers were also evaluated in flow through adsorption tests. In each test metals were placed into a saline solution to simulate tidal washing of storm sewers and adsorption break through curves were determined.

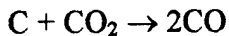
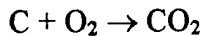
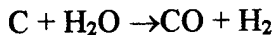
## Chapter 2

### BACKGROUND

#### 2.1 CARBON ADSORBENTS

Granular activated carbon (GAC) is prepared from one of two sources, naturally occurring carbonaceous material or synthetic polymeric precursors. Both of these carbons undergo similar activation processes.

Large surface areas can be created for both types of source material through the process of activation. This process involves the oxidation of the carbon to form pores created by volatilization. Typically the activation process involves a gas phase reaction with steam, air and carbon dioxide. In the reactions below carbon is converted to CO and CO<sub>2</sub> and volatilized forming a porous structure.



The key to creating a good adsorbent is to make a substance capable of concentrating molecules from a bulk solution (adsorbate) onto the surface of the adsorbent. Good adsorbents have large surface areas, typically from 400 to 2000 m<sup>2</sup>/g. van der Waals forces attract the adsorbent to the adsorbate molecules (Jenkins, 1976).

### **2.1.1 Naturally Occurring Activated Carbons**

Activated carbon created from naturally occurring carbonaceous substances are in wide use throughout the world. One popular application is in the treatment of drinking water. The creation of activated carbon consists of two phases. In the first phase the carbon is heated in the absence of air to 600°C. This step is referred to as charring the carbon. The next phase the carbon is activated with steam and other chemicals at 1000°C. The carbon can be further treated by chemicals to give it special selectivity for specific contaminants. The activation process gives carbon a surface area of around 1000 m<sup>2</sup>/g. There are numerous sources of raw material which activated carbon can be made, two promising sources for heavy metal removal are peat and bone char.

#### **2.1.1.1 Peat**

The application of peat as an adsorbent is gaining in popularity because it is abundant, inexpensive, and possesses numerous attributes, which make it an effective adsorbent for a variety of contaminants including metals.

Peat is a young coal in the initial stages of coalification. Coalification is a process that begins with the degradation of biota in a waterlogged environment. Water acts as a preservative while microorganisms slowly oxidize the biota. These reactions result in peat containing a mixture of lignin, cellulose, and humic acids. These constituents contain surface functional groups such as alcohols, aldehydes, carboxylic acid, ketones

and phenolic hydroxides making peat very polar with an affinity for dissolved metals and polar organic molecules (Allen, 1996).

Dissolved metals are adsorbed onto peat primarily by complexation with peat's surface functional groups. Copper and zinc ions complex with the carbonyl and nitrile groups in peat. The major factor of metal adsorption in peat is the presence of humic acids. Dissolved metals such as  $\text{Cu}^{2+}$  and  $\text{Fe}^{3+}$  react with humic acids to form a chelate ring involving adjacent aromatic carboxy and phenolic groups (Allen, 1996).

Authors disagree on the role that humic acid plays in the adsorption of metal ions. Ong and Swanson (1966) found that dissolved humic acids will complex dissolved metal ions. However, when humic acids were stripped from the peat the  $\text{Cu}^{2+}$  adsorption increased. Consequently, adsorption of metals by humic acid chelation may not be the driving force. The increased adsorption capacity as explained by Ong and Swanson (1966) was due to an increased surface area in the peat, which resulted when the humic acids were removed. The attraction was caused by a negative surface charge on the peat and a positively charged metal ion (Ong and Swanson, 1966). Allen (1996) and Ong and Swanson (1966) both reported that as the surface area of peat decreases or as carbon coalification increases the adsorption capacity decreases. The order of decreasing adsorption capacity is peat, lignite, and coal.

### **2.1.1.2 Bone Char**

Bone char is a naturally occurring adsorbent that is obtained from the thermal destruction of bones at 900°C. This material has a high capacity for irreversible metal sorption. Metal sorption is believed to be facilitated by the phosphorous-based hydroxyapatite/metal association. While, the adsorption capacity of bone char is high, production costs cause bone char to be an expensive material (Allen, 1996).

### **2.1.2 Polymer Carbons**

Polymer carbons are a class of adsorbents which provides an alternative to granular activated carbon. The chemical composition, pore structure, and surface chemistry are different from activated carbons.

Polymer carbons can be separated into two groups depending on the degree of heat that the polymer is exposed to during carbonization. If the polymer is heated until it melts, it is termed a fused polymer. This type of polymer will exhibit graphite like properties and have a low surface area. Fused polymers do not make good adsorbents. If the polymer retains its bead like shape during carbonization they are termed charred polymers. This type of carbon shows promise as an adsorbent due to increased surface area.

Pore structures of polymer carbons are determined from the precursor polymer and its pre-treatment technique. A polymer with a well defined porous structure is better

to start with than a polymer with no pores because the volatile organics, which will form during pyrolysis, can exit the polymer via the existing pores.

Porous polymers are typically charred at a temperature between 700°C and 1300°C providing for optimum pore size.

#### 2.1.2.1 SupelCarb<sup>TM</sup>

Physical characteristics of Supelcarb<sup>TM</sup> are listed in *Table 2-1*. This polymer begins as a porous bead. The polymer is rinsed in an ion exchange resin, which serves to break the C-H bond and replace the H<sup>+</sup> with the ion exchange resin. The polymer bead is subjected to pyrolysis at a temperature of greater than 300°C but not more than 1200°C; the temperature at which the C-C bonds would coalesce and form graphite. The ion exchange resin controls the shrinkage of the pore sizes. The pyrolysis will continue to a temperature in excess of 500°C where the ion exchange resin is volatilized and all that remains are C-C bonds in a hybridized sp<sup>3</sup> orbital (Betz, 1998).

Supelcarb<sup>TM</sup> is essentially a homogenous carbon substance. The charred polymer carbon has a negative surface charge due to the sp<sup>3</sup> orbital and will adsorb metal cations by van der Waals forces.

Table 2-1: Physical characteristics of Supelcarb<sup>TM</sup> and Carboxen-1011<sup>TM</sup>.

| Polymer Carbon              | Nominal Diameter, $\mu\text{m}$ | Surface Area, $\text{m}^2/\text{g}$ | Pore Distribution <sup>1</sup> , $\text{g}/\text{cm}^3$ | Density $\rho_b$ , $\text{g}/\text{cm}^3$ |
|-----------------------------|---------------------------------|-------------------------------------|---|---|
| Supelcarb <sup>TM</sup>     | 400-800                         | 1000                                | 0.37 micropores<br>0.25 mesopores<br>0.27 macropores    | 0.46                                      |
| Carboxen-1011 <sup>TM</sup> | 400-800                         | 1000                                | 0.42 micropores<br>0.19 mesopores<br>0.27 macropores    | 0.44                                      |

<sup>1</sup>Measured by 5-point Ar BET adsorption.

### **2.1.2.2 Carboxen – 1011<sup>TM</sup>**

The physical characteristics for Carboxen-1011<sup>TM</sup> can be found in *Table 2-1*. Carboxen<sup>TM</sup> is created the same way as Supelcarb<sup>TM</sup> except the precursor polymer is created with through put pores instead of dead end pores as with Supelcarb<sup>TM</sup>.

### **2.1.3 Mesoporous Silica Materials with Functionalized Monolayers**

The key to creating an adsorption media that will attract metals is to alter the surface of the media making it more attractive to the metal. Introducing thiol groups to the adsorbent surface increased adsorption properties of mesoporous silica (Feng et al., 1997). The thiol functional group will complex the metal out of solution. In research conducted by Feng et al. (1997), functionalized mesoporous silica filled 76% of its adsorption sites with metal ions as determined by transmission electron microscopy.

This particular adsorption media is especially attuned to the removal of mercury by the thiol functional groups. In laboratory tests, a 6.2 ppm total mercury solution with a pH of 3, 7, and 9 was reduced for each pH to a final equilibrium concentration of 0.0008 ppm total mercury after a contact time of 24 hours. From these results the distribution coefficient,  $K_d$ , was measured to be 340,000  $\mu\text{g Hg/g sorbent}$  ( Feng et al., 1997).

## **2.2 Adsorption Mechanisms**

The chemical reaction for the adsorption of a metal onto a solid substance is described by:



Where M is the metal adsorbate, S is the solid adsorbent and MS is the metal-solid adsorbent complex. Adsorbate molecules are held on the surface of the adsorbent primarily by two mechanisms, chemisorption and physisorption. Chemisorption is usually described as a covalent bond between the sorbate and sorbent. Physisorption is described as a weak, usually reversible attraction between the adsorbate and adsorbent. In our evaluation of Supelcarb<sup>TM</sup> and Carboxen-1011<sup>TM</sup>, physical entrapment of the metal into internal pores was the dominant sorption mechanism (i.e., physisorption).

Mechanisms that are important in the physical adsorption processes are: van der Waals forces; solvents interacting with the adsorbate, and the mechanism in which a adsorbate molecule is moved from the bulk solution to the adsorption site. Finally, the development of a mass transfer zone within the bed of the adsorber by the adsorbate is important in judging the effectiveness of the adsorber under flow through conditions.

### **2.2.1 van der Waals Force**

Van der Waals Forces are weak attractive forces that are effective over short distances. The force varies in strength in proportion to  $1/d^7$  where d is the atomic

diameter or molecular diameter. The van der Waal forces result from rapidly fluctuating electron density in one molecule that causes a complimentary electrical moment in an adjacent molecule. This force is the cause of adsorption at interfacial surfaces. Van der Waals Forces are also referred to as dispersion forces because it is the cause of optical dispersion.

A depiction of van der Waal forces is shown in *Figure 2-1*, which demonstrates the interaction between an atom and a planar surface. As the distance between the atom and the surface decrease, the net attractive forces increase. The net attractive force is at its peak at separation of around 3.5 Å (Jenkins, 1976).

The depth of the potential energy well can vary depending on the materials involved. The energy well is the measure of how strongly the materials are attracted together. Typical values range from 3 to 15 kcal/mol (Jenkins, 1976) for adsorbed molecules. Each adsorbate molecule could realize a different net attractive force depending on the strength of the dipole.

Van der Waals forces decrease rapidly as the adsorbate molecule moves away from the planar surface (*Figure 2-1*). Consequently, the adsorbate molecule adjacent to the adsorbent experiences the maximum van der Waals forces. A second layer of adsorbate molecules would experience a much weaker van der Waals force. This would indicate that adsorption will usually be mono layer when van der Waals forces control adsorption.

### **2.2.2 Adsorption From Solution**

In a metal contaminated solution the metal contaminant is referred to as the adsorbate and the water is referred to as the solvent. Adsorbate and solvent molecules compete for adsorption sites. The tendency for an adsorbate to adsorb before the solvent depends on which molecule has the larger attractive force for the sorbent. In cases where adsorbents have an affinity for solvents, adsorption of the adsorbate will be limited. Activated carbons and polymeric carbons work well as adsorbents in water because only a low attractive force is required to displace the water from the surface (Jenkins, 1976) (i.e., the carbonaceous adsorbent has a low affinity for water).

The adsorbate must have a larger affinity for the surface of the adsorbent than the solvent for adsorption to be likely to occur. The solubility of the adsorbate to the solvent is directly proportional to the affinity of the adsorbate to solvent and inversely proportional to the adsorption capacity (Jenkins, 1976).

Solubility and adsorption capacity are important in systems with low mutual affinity like carbon and water. The van der Waals forces that result in one species being soluble in another are the same force that causes adsorption. Soluble species have strong van der Waals forces to keep the species in solution. For a solute to become adsorbed the adsorptive van der Waals force must overcome the force that is keeping the solute in solution. As a species becomes less soluble the force keeping the species in solution decreases, causing the force necessary for adsorption to also decrease. Because many metals are less soluble as the pH of a solution increases, and metal adsorption often increases as pH increases (to a point) (Reed et al., 1983).

### **2.2.3 Pore Diffusion**

For a molecule to be adsorbed it must move to the surface of the adsorbent; travel through a macropore, move into a micro pore, and adsorb at an appropriate site. The solute movements through the macropores are assumed to be at the same rate as the bulk fluid. The rate of mass transport through the macro pores is inversely proportional to the adsorbate concentration and square of the particle radius. An increase in macropore volume per carbon volume will increase the mass transport. As adsorbate molecular weight increases the rate of mass transport decreases (Snoeyink, 1990).

### **2.2.4 Quiescent Liquid – Solid Adsorption**

Quiescent liquid-solid adsorption is typical in sedimentation basins or batch reactors. In this system the solid adsorbent is suspended in a quiescent basin, the solute is transported to the boundary layer of water surrounding the adsorbent by diffusion, and the solute crosses the hydrodynamic boundary layer. The thickness of this boundary layer is inversely proportional to the velocity of the water flowing past the suspended adsorbent. Hence, the time for this step would be longer for quiescent liquids. Once the adsorbate crosses the hydrodynamic boundary it moves to an adsorption site by pore diffusion or surface diffusion. Pore diffusion is defined as molecular diffusion through the solution in the pores. Surface diffusion is the movement along the adsorbent surface after adsorption occurs. Once the solute is transported to an adsorption site an adsorption

bond is formed. The rate determining step in this process is usually one of the transport steps (Snoeyink, 1990).

### **2.2.5 Fixed Bed Adsorption**

A solution is forced through a packed bed of adsorbent in this adsorption process. The transport steps described for quiescent adsorption are the same for fixed bed adsorption.

The region of the bed in which adsorption takes place is called the mass transfer zone (MTZ) (*Figure 2-2*). The adsorbent behind the MTZ is saturated with the adsorbate so the concentration of the solution at this point equals the influent concentration. The adsorbent in front of the MTZ has not been exposed to the solute so the concentration of the solution here is zero. Inside the MTZ the concentration of the solution varies from the influent concentration,  $C_o$ , to zero. The length of the MTZ depends on the rate of adsorption and the flow rate. Factors that increase of rate of adsorption are higher temperatures, smaller carbon particle size, greater diffusion, and more adsorption capacity of the adsorbate. An increase in the rate of adsorption would result in a shorter MTZ (Snoeyink, 1990).

### **2.3 Metal Adsorption**

Microporous carbonaceous adsorbents when added to water develop a surface charge. This surface charge can be attributed to surface functional groups such as

phenols and carboxyl. A surface charge may also result due to the electron orbital of the adsorbate. Supelcarb<sup>TM</sup> and Carboxen-1011<sup>TM</sup> are manufactured to have a sp<sup>3</sup> orbital. The sp<sup>3</sup> hybrid orbital results in a negative surface charge (Betz, 1998). The existence of surface charges causes an electric double layer to be formed.

Adsorption of metal ions onto microporous carbons is dependent on the pH of the solution. Solution pH has been identified as the variable governing metal adsorption on to solids (Reed *et al.*, 1992). This is due to the surface charge of the adsorbent and the aquatic chemistry of the metal ion. Adsorption increases with the solution pH for metal ions in a ligand free system.

Metals that are complexed in a solution may or may not adsorb like a metal in a ligand free system. Factors affecting adsorption in a ligand free system are pH, ionic strength, the activity of the ligand involved, and the type of adsorbent. The presence of a ligand could result in a stronger or weaker adsorbent bond.

If there is more than one adsorbable metal cation, then the metal ions will compete for adsorption sites. The metal cation that will adsorb the most depends on the affinity of each metal to the adsorbate, activity of the metals, solution pH, number of surface sites and ionic strength. The ionic strength can effect metal chemistry and the structure of the electronic double layer, which surrounds the surface of the adsorbate (Reed *et al.*, 1992).

A tool used to analyze metal ion activity in quiescent conditions is the EPA model A Geochemical Assessment Model for Environmental Systems: Version 3.0 (MINTEQ). MINTEQ is a chemical equilibrium speciation model. This model is capable of

determining equilibrium metal concentrations with a specified adsorbent present (Allison et al., 1990). This model was used to evaluate experimental data.

#### **2.4 Storm Water Best Management Practices**

Review of the literature on general industry practices for storm water management provided considerable insight into the design of BMPs. BMPs are planned to help minimize pollution discharges during a given industry day-to-day operations (Ross, 1993; Dunn, 1995; and Line, 1996). The most common (and common sense) aspect of BMPs is to minimize the contact of storm water with contaminant sources. Whenever possible, processes which generate a significant amount of contaminants are enclosed, shrouded and/or separated from other activities. EPA's major concern with industry is associated with spent paint and abrasive blasting material.

Despite municipalities and industries best efforts at avoiding storm water contact with heavy metals, contact does occur and metals are invariably transported into storm water systems and subsequently discharged into receiving waters (Host, 1996). The EPA discovered during a national study in 1992 that storm water discharges and other non-point sources are responsible for 1/3 to 2/3 of existing and threatened impairments to the native waters (EPA, 1992). To prevent contaminated storm water from impairing the beneficial use of receiving waters, municipalities and industry implemented storm water treatment systems.

#### **2.4.1 Oil/Water Separators**

In-line storm water treatment systems are currently BMPs at several industrial sites. These systems primarily treat the storm water for the removal of oils, greases, and suspended solids. Oils and greases are usually removed in an in-line oil/water separator. This unit process works by skimming the oil and grease off the top of the storm water flows (*Figure 2-3*). Suspended solids can be removed by channeling the storm water into a settling pond. These unit processes are designed to be bypassed during high flow conditions. The heavy metal adsorber could be placed within the oil/water separator and remove metals from contaminated storm water flows during design flow storm water events. This unit process would have to have a weir that allowed storm water flows that exceeded the design storm flow to by pass the heavy metal adsorber.

#### **2.4.2 Storm Water Settling Basins**

Storm water settling basins are sometimes referred to as extended detention ponds. This is a basin designed to store some rainfall up to 48 hours after a storm event. The detention pond stores the water with a hydraulic control structure that restricts outlet discharge (*Figure 2-4*). Detention of storm water in this process has been shown to remove 90% of particulates when water is stored for 24 hours or more depending on the size and configuration of the detention pond (Dunn et al., 1995). In an urban storm water settling basin a submerged aerobic biological filter was added in series with a storm water

settling basin and achieved 90% particulate removal plus 27% to 67% removal of copper and zinc (Anderson et al., 1996).

#### **2.4.3 Peat Sand Filter**

A peat sand filter is a multi layered filter that strains first flush run off through a layer of grass, peat, and finally sand. These filters are effective in small parking lots and other urban areas. The filter provides good ground water protection where infiltration into soils is feasible.

In a peat sand filter the main pollutant removal mechanism is straining through the filter layers. Some nutrient removal is accomplished in the grass and peat layers. Peat sand filters are effective storm water treatment systems for urban water sheds of up to 10 acres. This technology is reported to remove up to 90% of trace metals in an urban watershed (Dunn et al., 1995). Peat sand filters are a good way to treat contaminated storm water due to run off from existing facilities.

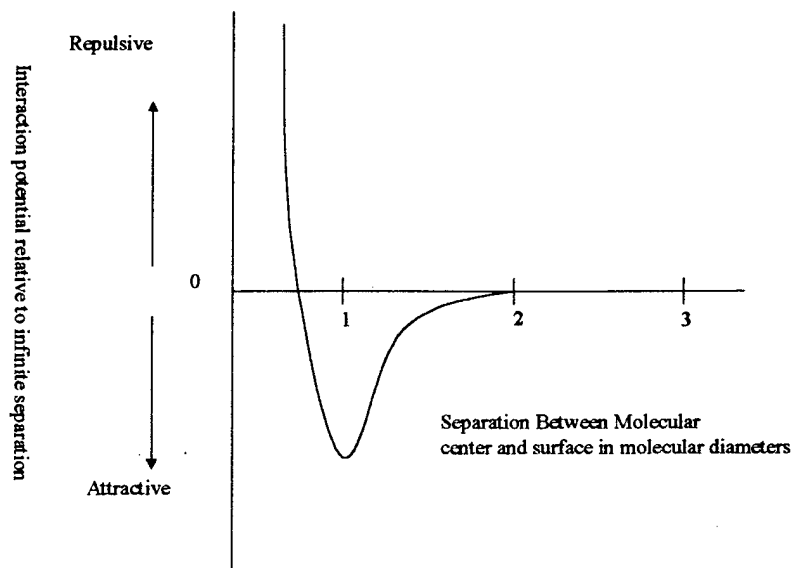


Figure 2-1: Typical van der Waals force between a molecule and a planar surface as a function of separation diameter (Jenkins, 1976).

---

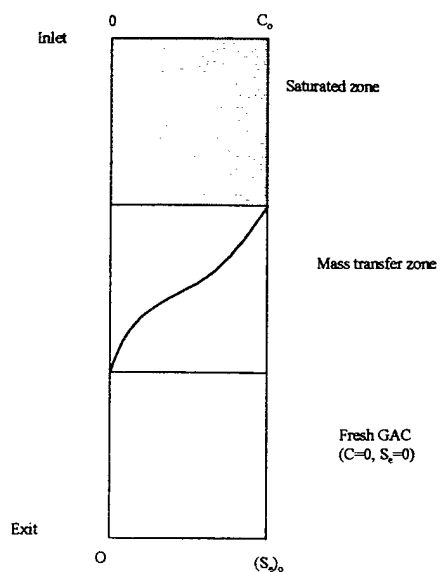
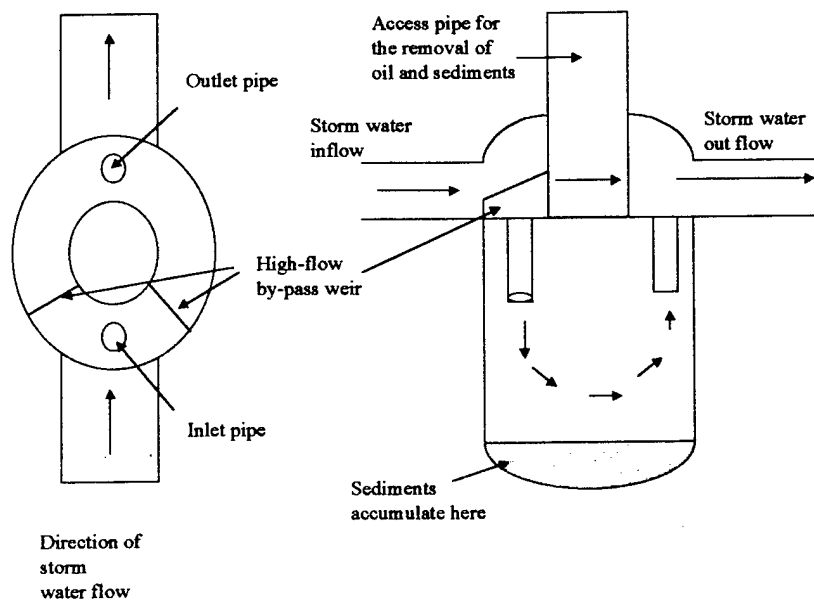
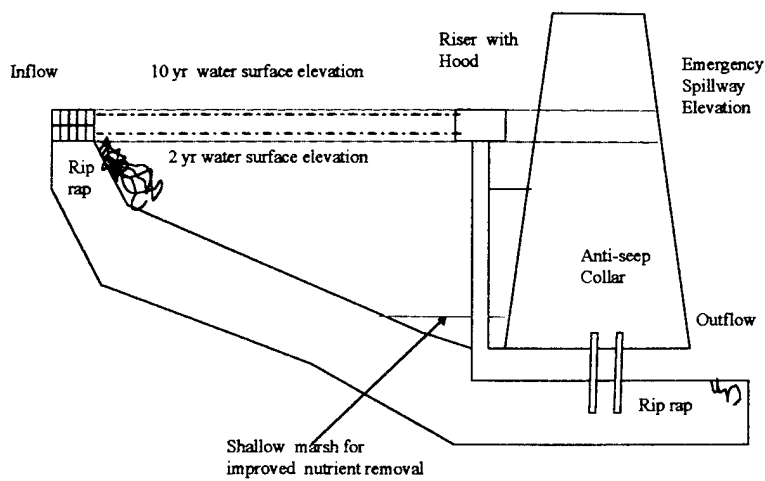


Figure 2-2: Adsorption column mass transfer zone (Snoeyink, 1990).

---



*Figure 2-3: Stormceptor™ oil/water separator plan and profile view. Storm water enters the upper chamber and goes to the lower chamber. Grit is deposited in the lower chamber and oils and greases will accumulate in the top. During high storm water flows most of the water by passes the lower chamber and exits the separator.*



*Figure 2-4: Stormwater settling basin (Dunn et al., 1995). Extended drainage ponds are effective for treating drainage water from 10 acres. This design has been shown to remove 60 to 80% of suspended solids.*

---

## Chapter 3

### METHODS AND MATERIALS

#### 3.1 Overview of the Test Program

Experiments were conducted to measure the adsorbent capacity and contaminant breakthrough characteristics of copper ( $Cu^{2+}$ ) and nickel ( $Ni^{2+}$ ) using two carbonaceous, charred porous polymer adsorbents, Supelcarb<sup>TM</sup> and Carbonex-1011<sup>TM</sup> (Supelco, Inc., Bellefonte, PA). The adsorbents have nearly identical physical properties (e.g., surface area, particle size and density) and essentially vary only in pore shape and pore size distribution. Batch adsorption experiments were conducted with both adsorbents to determine adsorption isotherms for  $Cu^{2+}$  and  $Ni^{2+}$  in a synthetic storm water solution of 100 mM NaCl, adjusted to pH  $6.3 \pm 0.2$  with 100 mM  $Na(HCO_3)_2$ . Flow through experiments, used to determine breakthrough characteristics, involved pumping synthetic storm water solutions containing single solute  $Cu^{2+}$  or  $Ni^{2+}$ , or bisolute  $Cu^{2+}$  and  $Ni^{2+}$  through an adsorbent cartridge (2.06 cm diameter, 7.8 cm bed depth) at bed velocities expected within storm water collection system. Influent and effluent concentrations were measured using atomic absorption spectrometry (AAS). Experimental variables included influent metal concentration (2.5 to 10 mg/L for  $Cu^{2+}$  and 1.25 to 5 mg/L for  $Ni^{2+}$ ) and

flow rate (100 to 300 mL/min). Influent metal concentrations used in experiments were 2-10 times higher than concentrations found in industrial locations (Line et al. 1996)

### **3.2 Materials**

#### **3.2.1 Adsorbents**

Adsorbents used in this experiment were charred porous polymers, Supelcarb<sup>TM</sup> and Carbonex-1011<sup>TM</sup>, manufactured by Supelco, Inc. of Bellefonte, PA. The adsorbents were selected for their unique pore shapes and pore size distribution. Supelcarb<sup>TM</sup> is characterized by “dead end” pores; pores, which are funnel shaped and do not transfix the particle’s core. Carboxen-1011<sup>TM</sup> adsorbent pores pierce the particle’s core in an “hour glass” shape. Physical characteristics of the two adsorbents are listed in *Table 3-1*.

#### **3.2.2 Synthetic Storm water Solutions**

All experiments used a synthetic storm water of 100 mM NaCl to maintain ionic strength. A constant pH was maintained by using 100 mM NaHCO<sub>3</sub> as a buffer. The pH was adjusted with 100 mM NaOH or 100 mM HCl. The procedures used are outlined below:

---

Table 3-1: Physical characteristics of Supelcarb™ and Carboxen-1011™

| Adsorbent      | Shape  | Diameter<br>( $\mu\text{m}$ ) | Bulk<br>Density<br>(g/cc) | Porosity                      |                                 |                                |
|----------------|--------|-------------------------------|---------------------------|-------------------------------|---------------------------------|--------------------------------|
|                |        |                               |                           | Micro<br>( $<10\mu\text{m}$ ) | Meso<br>(10-100 $\mu\text{m}$ ) | Macro<br>( $>100\mu\text{m}$ ) |
| Supelcarb™     | sphere | 400-800                       | 0.46                      | 0.37                          | 0.25                            | 0.27                           |
| Carboxen-1011™ | sphere | 400-800                       | 0.44                      | 0.42                          | 0.19                            | 0.27                           |

---

### **3.2.2.1 Stock Solutions**

#### **3.2.2.1.1 Rinse and Dilution for the Influent Solutions: 100mM NaCl with pH Buffer.**

1. Weigh out 116.886 g of “Ultra Pure” NaCl (J.T. Baker) on a Delta Range® Mettler Balance, Model AG204;
2. measure 50 mL of 100 mM Na(HCO<sub>3</sub>)<sub>2</sub> (Fisher Scientific) in a class A, volumetric flask and place into an acid washed 28 L Nalgene™ container, as a pH buffer;
3. dissolve the NaCl with 4 L of de-ionized water in a 4 L Erlenmyer flask;
4. pour the solution into the Nalgene™ container;
5. use the 4 L Erlenmyer Flask to add 16 L of de-ionized water; for a total of 20.05 L, 100 mM NaCl.

#### **3.2.2.1.2 Dilution for Stock Solutions: 100 mM NaCl without pH Buffer**

1. Weigh out 116.886 g of “Ultra Pure” NaCl (J.T. Baker) on a Delta Range® Mettler Balance, Model AG204;
2. dissolve the NaCl with 4 L of de-ionized water in a 4 L Erlenmyer flask;
3. pour the solution into the Nalgene™ container;
4. use the 4 L Erlenmyer Flask to add 16 L of de-ionized water; for a total of 20 L, 100 mM NaCl.

**3.2.2.1.3 Stock Solution: 5000 mg Cu<sup>2+</sup>/L**

1. In an acid washed 1000 mL, class A, volumetric flask, add 5 mL of 50% Nitric Acid (VWR) (1 + 1 HNO<sub>3</sub>) as a preservative;
2. weigh out 13.4107 g of CuCl<sub>2</sub>•2H<sub>2</sub>O (Fisher Scientific) on a Delta Range® Mettler Balance, Model AG204;
3. add the 13.4107 g of CuCl<sub>2</sub>•2H<sub>2</sub>O to the flask;
4. dilute to 1000 mL with unbuffered stock dilution solution.

**3.2.2.1.4 Stock Solution: 10 mg Cu<sup>2+</sup>/L**

1. Pipette one milliliter of 5000 mg Cu<sup>2+</sup>/L stock solution into an acid washed, 500 mL, class A, volumetric flask;
2. fill to 500 mL with buffered stock dilution solution.

**3.2.2.1.5 Stock Solution: 1000 mg Ni<sup>2+</sup>/L**

1. In an acid washed 1000 mL, class A, volumetric flask, add 5mL of 50% Nitric Acid (VWR) (1 + 1 HNO<sub>3</sub>) as a preservative;
2. weigh out 4.0472 g of “Baker Analyzed®” NiCl<sub>2</sub>•6H<sub>2</sub>O (J.T. Baker) on a Delta Range® Mettler Balance, Model AG204;
3. add the 4.0472 g of NiCl<sub>2</sub>•6H<sub>2</sub>O to the flask;
4. dilute to 1000 mL with unbuffered stock dilution solution.

### **3.2.2.1.6 Stock Solution: 10 mg Ni<sup>2+</sup>/L**

1. Pipette 5 mL of 1000 mg Ni<sup>2+</sup>/L stock solution into an acid washed, 500 mL, class A, volumetric flask;
2. fill to 500 mL with buffered stock dilution solution.

### **3.2.2.2 Batch Experiment Solutions**

1. For the desired influent concentration, the amount shown in *Table 3-2*, was added to an acid washed, 200 mL, class A volumetric flask;
2. add buffered stock dilution solution until approximately two-thirds full;
3. check pH with a Beckman ø 31 pH meter and adjust to pH of  $6.3 \pm 0.2$  with 100 mM Na(HCO<sub>3</sub>)<sub>2</sub> (Fisher Scientific);
4. fill to 200 mL with buffered stock dilution solution.

### **3.2.2.3 Flow Through Experiment Solutions:**

1. For the desired influent concentration, the amount shown in *Table 3-3* was added to an acid washed, 20 L, Nalgene™ container;
2. fill to 20 L with buffered stock dilution solution.

*Table 3–2:* Volume of stock solution for a desired influent concentration used in the batch experiments.  $V_T = 200$  mL.

| Metal Ion Concentration (mg $M^{2+}$ /L) | Volume of 10 mg $Cu^{2+}$ /L (mL) | Volume of 5000 mg $Cu^{2+}$ /L (mL) | Volume of 10 mg $Ni^{2+}$ /L (mL) | Volume of 1000 mg $Ni^{2+}$ /L (mL) |
|--|-----------------------------------|-------------------------------------|-----------------------------------|-------------------------------------|
| 1.25                                     | 25                                | 0                                   | 25                                | 0                                   |
| 2.5                                      | 50                                | 0                                   | 50                                | 0                                   |
| 5  | 100                               | 0                                   | 100                               | 0                                   |
| 10                                       | 200                               | 0                                   | 200                               | 0                                   |
| 25                                       | 0                                 | 1                                   | 0                                 | 5                                   |
| 50                                       | 0                                 | 2                                   | 0                                 | 10                                  |
| 100                                      | 0                                 | 4                                   | 0                                 | 20                                  |

*Table 3-3: Volume of stock solution for a desired influent concentration used in the flow through experiments.  $V_T = 20 \text{ L}$*

| Experimental Concentration (mg Cu <sup>2+</sup> /L) | Experimental Concentration (mg Ni <sup>2+</sup> /L) | Volume of 5000 mg Cu <sup>2+</sup> /L (mL) | Volume of 1000 mg Ni <sup>2+</sup> /L (mL) | Mass of NiCl <sub>2</sub> (g) |
|---|---|--|--|-------------------------------|
| 2.5   | 0   | 10   | 0  | 0                             |
| 5.0   | 0   | 20   | 0  | 0                             |
| 10.0  | 0   | 40   | 0  | 0                             |
| 0   | 1.25  | 0  | 25   | 0                             |
| 0   | 2.0   | 0  | 40   | 0                             |
| 0   | 5.0   | 0  | 100  | 0                             |
| 5   | 4.62  | 20   | 0  | 0.3740                        |
| 10  | 4.62  | 40   | 0  | 0.3740                        |
| 5   | 9.24  | 20   | 0  | 0.7479                        |

### **3.3 Experimental Methods**

All experiments described below were conducted in triplicate to balance statistical reliability, budget and schedule restrictions.

#### **3.3.1 Batch Experiments**

Batch experiments were conducted to evaluate adsorption isotherms for Cu<sup>2+</sup> and Ni<sup>2+</sup> at a constant ionic strength of 0.1 M to simulate tidal washed storm sewer environment. The experiment involved a 250 mL beaker as a reactor vessel containing 200 mL of the metal spiked synthetic storm water solution, and 1 gram (dry weight) of adsorbent. Once combined, the reactor contents were continuously mixed, using a Teflon™ magnetic stir bar on a Challenge Environmental Systems, Model MS8-300, 8-position magnetic stirring plate, for ten minutes. A ten minute contact time was selected to approximate the maximum residence time of storm water in a in-line adsorbent cartridge placed into an existing storm water treatment system. After ten minutes, the adsorbent and solution were separated using a 0.45 µm Analytical Filter Unit (Nalgene™, CN, Model 130-4045). The pH of the solution was adjusted to less than 2.0 by adding one to two drops of concentrated nitric acid. The influent and effluent concentrations were measured using a Perkin-Elmer™, Model 3030 B, Atomic Absorption Spectrometer (AAS). The procedures used are outlined below:

1. Prepare in triplicate the eight influent concentrations (Table 3-2) in separate 250 mL beakers;
2. remove 1 mL from each reactor and place in separate, acid washed, 25 mL, class A, volumetric flasks;
3. to each 25 mL flask add one drop of concentrated nitric acid;
4. fill with buffered stock dilution solution and set aside;
5. in the remaining 250 mL reactors, place an acid washed Teflon™ magnetic stir bar and place on a Challenge Environmental Systems, Model MS8-300, 8-position magnetic stirring plate;
6. to each reactor, add 1 gram of adsorbent (previously weighed on a Delta Range® Mettler Balance, Model AG204) and let mix for ten minutes;
7. after ten minutes, separate the adsorbent from the solution using a 0.45 $\mu$ m Analytical Filter Unit (Nalgene™, CN, Model 130-4045);
8. measure the pH of each filtered solution with a Beckman ø 31 pH meter;
9. add one to two drops of concentrated nitric acid (VWR) to eight clean, acid washed, 250 mL beakers;
10. place the filtered solution from each sample in separate beakers;
11. measure the pH in each beaker, with a Beckman ø 31 pH meter, to ensure it is below 2.0;
12. measure the influent and effluent concentrations using the AAS.

### **3.3.2 Flow Through Experiments**

Flow through experiments were conducted to determine the effects of varying mass flow rates on sorption and contaminant breakthrough. Influent solutions, of varying metal concentration, were pumped at constant flow rates through an in-line 0.45  $\mu\text{m}$  filter (Gelman<sup>TM</sup>, Model 12178) and a one-inch diameter column containing  $12.0 \pm 0.1$  grams of tightly packed adsorbent (*Figure 3-1*).

The column discharged to two mixing basins in series. The first basin served as a port to monitor outlet pH. The second basin served as a mixing port for a slow continuous titration of concentrated nitric acid to maintain pH less than 2.0 and as a sampling port where concentrations could be measured by AAS at one minute intervals. "Breakthrough" was defined as the point where the effluent concentration equaled 10% of the influent concentration. Once the 10% criteria was attained, the influent was switched to a rinse of metal free synthetic storm water solution, for ten minutes. Measurements were taken every minute during rinsing to evaluate if any desorption occurred. The procedures used are outlined below:

1. Cut a six inch length of one inch O.D. stainless steel tube ( $^{13}/_{16}$  inch I.D.) and fit one end with Swagelok<sup>TM</sup> reducing unions from 1 inch to  $^{3}/_{8}$  inch;
2. using a  $\frac{1}{2}$  inch stainless steel rod, pack the column with approximately  $\frac{1}{2}$  inch of glass wool;
3. weigh out  $12.0 \pm 0.1$  g of adsorbent on a Delta Range<sup>®</sup> Mettler Balance, Model AG204;
4. pour 25% of the adsorbent into the column;

5. compact the adsorbent by “rodding” it 24 times with the stainless steel rod;
6. repeat steps 4 and 5 three more times;
7. tightly pack the remainder of the column with glass wool;
8. close the column with another set of Swagelok™ reducing unions from 1 inch to  $\frac{3}{8}$  inch;
9. set up experimental apparatus as shown in *Figure 3-2*;
10. prepare 20 L of rinse solution;
11. prepare 20 L of metal-spiked synthetic storm water solution (*Table 3-3*);
12. measure the concentration of metal ions in the influent by AAS;
13. pump metal-free rinse until the desired flow rate (100, 200, or 300 mL/min) is achieved, using the Master Flex® L/S™ Variable-Speed Modular Drive with L/S™ 18 pump head;
14. adjust the concentrated nitric acid (VWR) “drip” to maintain pH <2 in the sampling basin;
15. place the AAS aspirator at the outlet of the sampling basin;
16. switch inlet flow from rinse to spiked influent solution;
17. start timer;
18. take initial AAS reading;
19. take AAS readings at one minute intervals;
20. when AAS readings indicate effluent concentration  $\geq 10\%$  of influent, switch influent back to rinse;
21. continue rinse for ten minutes or until effluent concentration returns to zero.

### **3.4 Analytical Methods**

#### **3.4.1 Atomic Absorption Spectrometry**

Metal ion concentrations were measured on a Perkin-Elmer™, Model 3030 B, AAS, with a Perkin-Elmer™, PR-100 Printer for data capture. AAS utilizes absorption of ultra violet or visible radiation to determine the concentration of samples. The schematic diagram of the AAS is shown in *Figure 3-3*.

At the light source, an electric potential is introduced between the cathode and the anode, energizing a hollow cathode lamp consisting of an anode and a metal specific cathode. The potential difference causes electrons to strike the cathode, resulting in “sputtered” metal ions some with electrons elevated to excited orbitals. The excited electrons fall back into the “ground state”, sending light at a unique wavelength,  $\lambda \pm 0.01\text{nm}$ , through the flame, which contains sample metal ions in the ground electronic state. The light source is mechanically chopped to create a double beam, one beam going through the flame and the other around the flame.

A small portion of the sample is aspirated into the flame. This sample is made into an aerosol and then converted to gaseous elementary particles. This process is referred to as vaporization. The atomized sample will absorb light in direct proportion to its concentration. The remaining light will pass to the monochromator, dispersing it and sending a specific wavelength of light to the detector. The detector will convert the light it absorbs into an electronic signal. The auto calibration feature on this machine will take

the absorbence reading and apply it to a standard curve of absorbence versus concentration. The concentration can now be viewed on the AAS computer screen.

All samples were filtered, using a 0.45  $\mu\text{m}$  filter, then acidified to a pH < 2.0 in accordance with Standard Methods, 313A for  $\text{Cu}^{2+}$  and 321 for  $\text{Ni}^{2+}$  (APHA 1985). Acidification prevents the metal from adsorbing to the sides of the container, as metals are more soluble at low pH's. Additionally, acidification dissolves most  $\text{Cu}^{2+}$  and  $\text{Ni}^{2+}$  precipitates, especially oxy-hydroxide and carbonates.

### **3.4.2 AAS Calibration**

The AAS required calibration prior to measuring the influent and effluent concentrations in each experiment. The AAS was calibrated by comparing solutions of known concentration and ionic strength to the measured absorbence. Since the AAS measured absorbence is directly proportional to the concentration, within a limited range, the concentration can be derived from the slope ( $m$ ) and intercept ( $b$ ) of the calibration curve. The calibration curve compares measured absorbence against known concentrations. The AAS allows the operator the option to auto-zero the instrument to establish a benchmark reading from which all subsequent readings are relative. The auto-zero function was utilized for the 0 mg/L calibration solution. Therefore, the value of the y intercept ( $b$ ) is 0 for every calibration curve. *Figure 3-4* is a representative calibration curve and shows the constants for calculating experimental concentrations from measured absorbances.

### **3.4.2.1 Calibration Solutions for Cu<sup>2+</sup>**

The AAS was calibrated using solutions of: 0, 1, 2, 3, 4 and 5 mg Cu<sup>2+</sup>/L. The procedure is described below:

### **3.4.2.2 Calibration Solution: 1 mg Cu<sup>2+</sup>/L**

1. In an acid washed 1000 mL, class A, volumetric flask, add 5 mL of 50% Nitric Acid (VWR) (1 + 1 HNO<sub>3</sub>) as a preservative;
2. pipette 1 mL of 1000 mg/L Atomic Absorption Standard (E.M. Scientific);
3. weigh out 5.8443 g of "Ultra Pure" NaCl (J.T. Baker) on a Delta Range® Mettler Balance, Model AG204;
4. add the 5.8443 g of "Ultra Pure" NaCl (J.T. Baker) to the flask;
5. dilute to 1000 mL with Milli-Q™ de-ionized water (Millipore);
6. repeat steps 1 through 5 four times, each time increasing the volume of Atomic Absorption Standard by 1 mL.
7. repeat steps 1 through 5, omitting step 2, to make the 0 mg Cu<sup>2+</sup>/L calibration solution.

### **3.4.2.3 Calibration Solution for Ni<sup>2+</sup>**

The AAS was calibrated using solutions of: 0, 0.5, 1, 1.5, and 2 mg Ni<sup>2+</sup>/L. The procedure is described below:

#### **3.4.2.4 Calibration Solution: 0.5 mg Ni<sup>2+</sup>/L**

1. In an acid washed 200 mL, class A, volumetric flask pipette 1 mL of 1000 mg/L Atomic Absorption Standard (J.T. Baker);
2. dilute to 200 mL with unbuffered stock solution dilution to make a 5 mg Ni<sup>2+</sup>/L solution;
3. In an acid washed 1000 mL, class A, volumetric flask, add 5 mL of 50% Nitric Acid (VWR) (1 + 1 HNO<sub>3</sub>) as a preservative;
4. add 100 mL of 5 mg Ni<sup>2+</sup>/L;
5. weigh out 5.8443 g of “Ultra Pure” NaCl (J.T. Baker) on a Delta Range® Mettler Balance, Model AG204;
6. add the 5.8443 g of “Ultra Pure” NaCl (J.T. Baker) to the flask;
8. dilute to 1000 mL with Milli-Q™ de-ionized water (Millipore);
9. for the 1.5 mg Ni<sup>2+</sup>/L solutions, repeat steps 1 through 6, increasing the volume of Atomic Absorption Standard in step 1 to 3 mL.
10. for the 1 and 2 mg Ni<sup>2+</sup>/L solutions, follow the procedure outlined in section 3.4.2.2, substituting AAS Nickel Standard for Copper.
10. repeat steps 3 through 7, omitting step 4, to make the 0 mg Ni<sup>2+</sup>/L calibration solution.

### **3.5 Data Reduction**

Data captured from an experiment, in the form of measured absorbences (MA), were converted to experimental concentrations using the following formula:

$$C = m * MA + b \quad (3-1)$$

where:

C = concentration of metal ions on a mass per volume basis,

m = slope of the calibration curve,

MA = AAS measured absorbance of sample,

b = y intercept of the calibration curve (= 0 due to auto-zero feature of AAS).

Once the influent and effluent concentrations were calculated, the data were reduced to their reported form depending on the test type, batch or kinetic. The procedures for handling data from both types of experiments are described below:

#### **3.5.1 Batch Data Handling**

1. Subtract the final concentration from the initial,

$$C_{\delta} = C_i - C_f \quad (3-2)$$

where:

$C_{\delta}$  = concentration of metal ions removed (mg/L),

$C_i$  = initial concentration of metal ions (mg/L),

$C_f$  = final concentration of metal ions (mg/L);

2. multiply the difference in concentrations by the volume of solution to get mass of metal ions removed:

$$M_\delta = C_\delta * V \quad (3-3)$$

where:

$M_\delta$  = mass of metal ions removed (mg),

$C_\delta$  = concentration of metal ions removed (mg/L),

$V$  = volume of solution (L);

3. divide the mass of metal ions removed by the mass of adsorbent in the reactor:

$$S = M_\delta / M_{ads} \quad (3-4)$$

where:

$S$  = mass of metal ions sorbed per mass of adsorbent (mg  $M^{2+}$ /g adsorbent),

$M_{ads}$  = mass of adsorbent in the reactor (g);

4. plot the final concentration of metal ions ( $C_f$ ) versus sorbed concentration ( $S$ );

5. calculate  $K_f$  and  $n$  using the Freundlich Equation (Schwarzenbach et al, 1993):

$$S = K_f * C_f^n \quad (3-5)$$

where:

$S$  = Sorbed concentration (mg  $M^{2+}$ /g adsorbent),

$C_f$  = dissolved concentration (mg  $M^{2+}$ /L),

$K_f$  = Freundlich distribution coefficient  $(L/g)^{1/n}$ ,

$n$  = Freundlich measure of non-linearity.

The capacity of the adsorber is described by  $K_f$ . If  $C_f$  and  $n$  are held constant then  $S$  increases proportionally to  $K_f$ . The term  $n$  describes the strength of the adsorption

bond. For example, when  $K_f$  and  $C_f$  are held constant, decreasing values of  $n$  have a reduced effect on  $S$ . Smaller values of  $n$  represent stronger adsorption bonds and increased irreversibility of the reaction. Likewise, larger values of  $n$  indicate weaker adsorption bonds and increase the sensitivity of  $S$  to small changes in  $C_f$  (Snoeyink 1990). For these reasons, the Freundlich adsorption isotherm constants provide a practical basis for evaluating the performance of an adsorbing media.

### **3.5.2 Flow Through Data Handling**

1. Divide the effluent concentrations by the influent concentration to get the ratio of effluent to influent concentration,

$$C_i \div C_f = C_\infty \quad (3-6);$$

2. calculate the empty bed contact time (EBCT) for the adsorbent column

$$EBCT = (\text{Volume of Adsorbent, mL}) / (\text{Rate of Flow, mL/min}) \quad (3-7)$$

3. calculate number of bed volumes (BV)

$$BV = (\text{Time at } C_\infty, \text{ min}) / EBCT \quad (3-8)$$

4. plot the number of bed volumes to breakthrough, (BV) vs. the effluent ratio ( $C_\infty$ ),

through  $C_\infty = 0.10$ ;

5. from the graph determine the number of bed volumes for each experiment to reach  $C_\infty = 0.02, 0.04, 0.06, 0.08$  and  $0.10$ ;

6. average the number of bed volumes to break through for the three experiments and develop a composite number of bed volumes to breakthrough curve;

7. in experiments where an effluent ratio is observed at more than one number of bed volumes, the averaged value is used for the composite graph;
8. *Figure 3-5* and *Figure 3-6* illustrate the procedure outlined above.

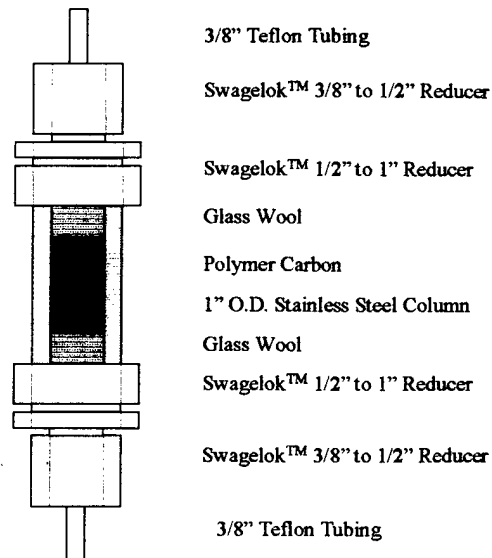


Figure 3-1: Elevation view of a typical adsorbent column (Snoeyink, 1990).

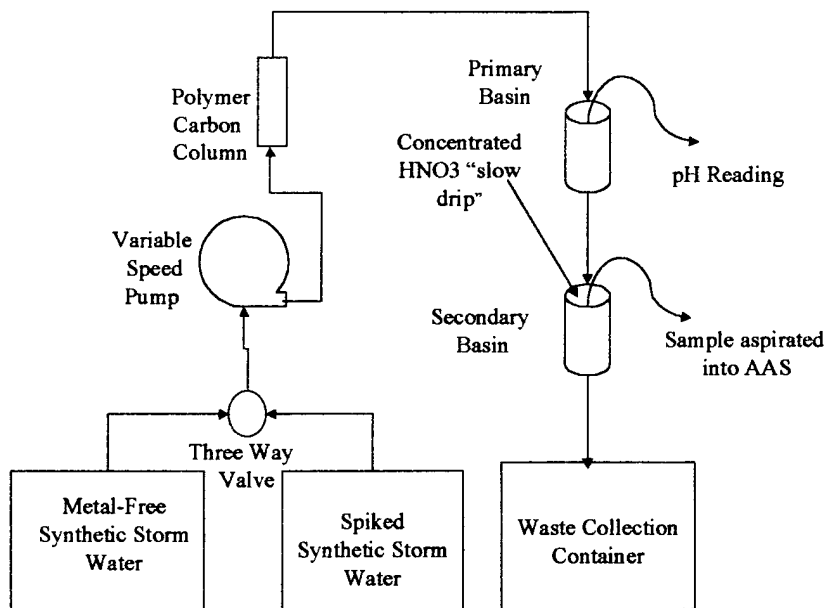


Figure 3-2: Schematic of experimental apparatus for the flow through tests.

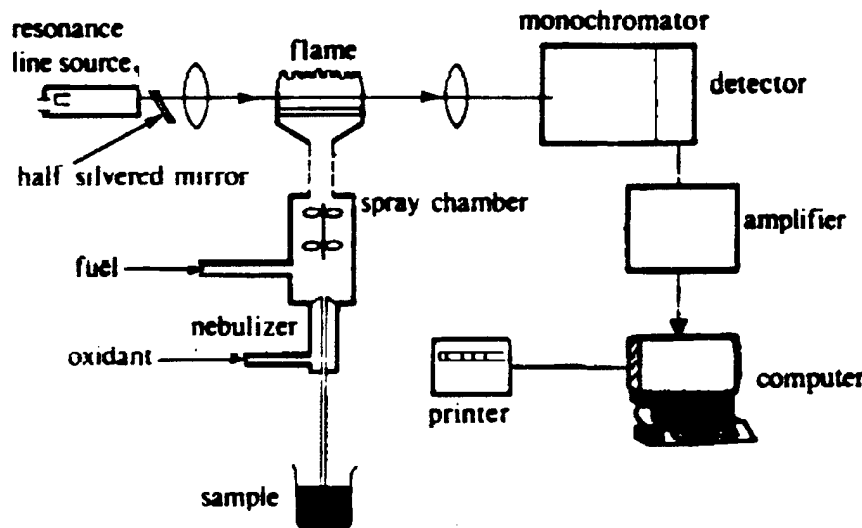


Figure 3-3: Single beam atomic absorption spectrometer (Fifield and Haines, 1995).

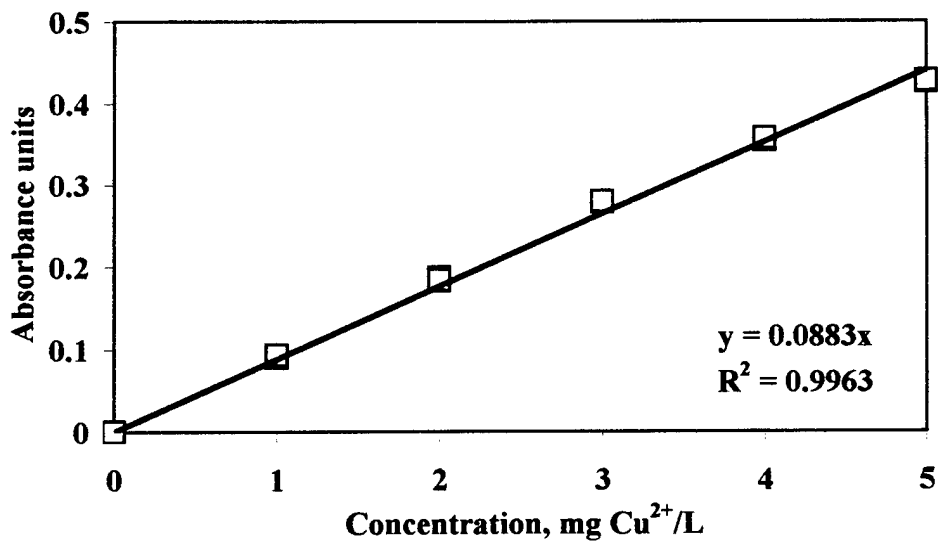


Figure 3-4: Representative AAS calibration curve.

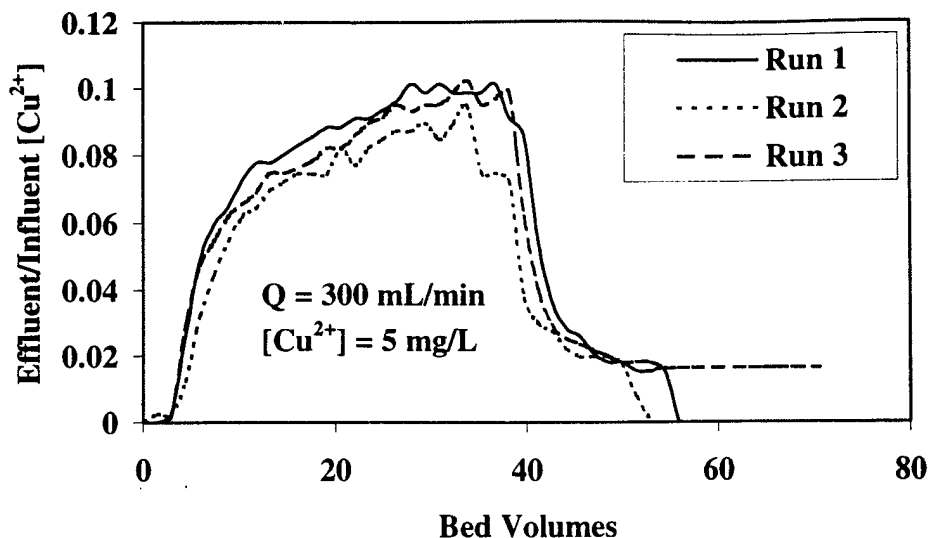


Figure 3-5: Sample bed volume to breakthrough curve showing triplicate sets of one experimental condition. The graph illustrates that there is no de-adsorption of copper in this experimental condition.

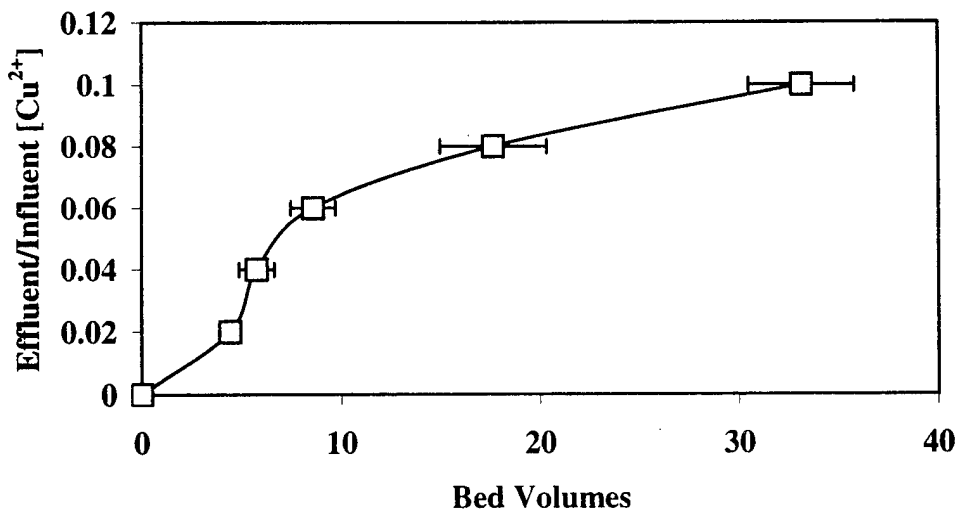


Figure 3-6: Average bed volumes to break through curve showing the reduction of triplicate data sets to one average break through curve. The graph illustrates that there is no de-adsorption of copper in this experimental condition.

## Chapter 4

### RESULTS AND DISCUSSION

The objective of this research was to determine the effectiveness of two commercially available charred porous polymers to remove dissolved heavy metals in storm water. The performance of the two charred porous polymers was analyzed under two distinct experimental conditions, batch and flow through. The flow through experiments were further divided into two phases; adsorption of a single dissolved metal and adsorption of two dissolved metals (bisolute). Quantitative measurements of the concentrations of dissolved metal(s), in both influent and effluent solutions, were made by AAS.

#### 4.1 Results

##### 4.1.1 Cu<sup>2+</sup> in Synthetic Storm Water

###### 4.1.1.1 Batch Results for Cu<sup>2+</sup>

Results of the batch experiments for Cu<sup>2+</sup> are presented in *Figure 4-1* and *Figure 4-2*. For each charred porous polymer the mass of Cu<sup>2+</sup> sorbed per mass of sorbent is

plotted versus the effluent concentration. As discussed in Section 3.3, triplicate tests were conducted on each of eight influent concentrations. The samples were continually mixed for ten minutes. After ten minutes, the samples were filtered, the supernant was acidified with concentrated nitric acid, and the concentration of  $\text{Cu}^{2+}$  in the effluent determined by AAS.

The results indicate total removal of  $\text{Cu}^{2+}$  in influent concentrations of 10 mg/L, or less. The convex shape of the data in both figures indicates the Freundlich constant,  $n$ , is less than 1 for both adsorbents (Schwarzanback, et. al., 1993), which suggests strong adsorption bonds (Snoeyink, 1990).

*Figure 4-1* and *Figure 4-2* also indicate the adsorption capacities ( $S_{\max}$ ) for each charred porous polymer. *Figure 4-1* shows Supelcarb™ with a  $S_{\max}$  of 11 mg  $\text{Cu}^{2+}$ /g adsorbent, while *Figure 4-2* shows 12 mg  $\text{Cu}^{2+}$ /g adsorbent for Carboxen-1011™.  $S_{\max}$  is the asymptotic maximum sorbed concentration of the isotherm.

Freundlich constants are calculated from the slope, which represents  $n$ , and the y-intercept, representing  $K_f$ , of the plot of the natural log,  $\ln$ , of the mass  $\text{Cu}^{2+}$  sorbed per gram of adsorbent,  $\ln S$ , versus the natural log,  $\ln$ , of the effluent concentration,  $\ln C$ .

*Figure 4-3* represents the plot of  $\ln S$  versus  $\ln C$  for Supelcarb™ and is typical of the method used to calculate Freundlich constants, which are listed in *Table 4-1*.

---

Table 4-1: Summary of Freundlich adsorption isotherm coefficients for Supelcarb™ and Carboxen-1011™ from batch experiments with Cu<sup>2+</sup> in synthetic storm water.

| Charred Porous Polymer | Freundlich Coefficients             |      |
|------------------------|-------------------------------------|------|
|                        | K <sub>d</sub> (L/g) <sup>1/n</sup> | n    |
| Supelcarb™             | 3.07                                | 0.31 |
| Carboxen – 1011™       | 5.31                                | 0.20 |

---

#### **4.1.1.2 Flow Through Results for Cu<sup>2+</sup>**

Results of the flow through experiments for Cu<sup>2+</sup> in the synthetic storm water solution are presented in *Figure 4-4* through *Figure 4-7*. For each charred porous polymer, the effluent concentrations, as a percent of the influent concentrations, are plotted versus bed volumes. As discussed in Section 3.3, triplicate tests were conducted at each concentration for each flow setting. The results demonstrate that both charred porous polymers remove Cu<sup>2+</sup> from synthetic storm water at low flow rates. Both polymers exhibited approximately linear relationships between effluent concentration and bed volume, above the first measurable Cu<sup>2+</sup> concentration until break through. The results also indicate disproportionate responses to increases in flow, but not to increases in concentration. For example, doubling the flow from 100 mL/min to 200 mL/min, reduced the Cu<sup>2+</sup> number of bed volumes to break through by 75% to 85%, doubling the concentration from 2.5 mg Cu<sup>2+</sup>/L to 5 mg Cu<sup>2+</sup>/L reduced Cu<sup>2+</sup> number of bed volumes to breakthrough by 10% to 25%.

#### **4.1.2 Ni<sup>2+</sup> in Synthetic Storm Water**

##### **4.1.2.1 Batch Results for Ni<sup>2+</sup>**

Results of the batch experiments for Ni<sup>2+</sup> in synthetic storm water solution are presented in *Figure 4-8* and *Figure 4-9*. As in *Figures 4-1* and *4-2*, the mass Ni<sup>2+</sup> per mass of sorbent is plotted, for each charred porous polymer, versus the effluent concentration. The results indicate that these charred porous polymers did not appreciably remove Ni<sup>2+</sup>. *Table 4-2* summarizes the Freundlich adsorption constants for Ni<sup>2+</sup> in synthetic storm water solution. *Figures 4-14* and *4-15* also show S<sub>max</sub> for Supelcarb<sup>TM</sup> of 0.13 mg Ni<sup>2+</sup>/g and 1.8 mg Ni<sup>2+</sup>/g for Carboxen-1011<sup>TM</sup>.

##### **4.1.2.2 Flow through Results for Ni<sup>2+</sup>**

Results of the flow through experiments for Ni<sup>2+</sup> in synthetic storm water solution are presented in *Figure 4-10* and *Figure 4-11*. For each charred porous polymer, the effluent concentrations, as a percent of the influent concentrations, are plotted versus bed volumes. Triplicate tests were conducted at a constant flow rate of 200 mL/min. As with the batch experiments, the charred porous polymers were ineffective at removing Ni<sup>2+</sup> from synthetic storm water.

---

Table 4-2: Summary of Freundlich adsorption isotherm coefficients for Carboxen-1011™ from Ni<sup>2+</sup> batch experiments.

| Charred Porous Polymer | Freundlich Coefficients |       |
|------------------------|-------------------------|-------|
|                        | $K_d (L/g)^{1/n}$       | n     |
| Supelcarb™             | 0.122                   | 0.058 |
| Carboxen – 1011™       | 0.621                   | 0.27  |

---

#### **4.1.3 Competitive Adsorption Flow Through Results for Cu<sup>2+</sup> and Ni<sup>2+</sup>**

Results of the flow through experiments for Cu<sup>2+</sup> and Ni<sup>2+</sup> in the synthetic storm water solution are presented in *Figure 4-12* and *Figure 4-13*. For each charred porous polymer, the effluent concentrations, as a percentage of the influent concentrations, are plotted versus bed volume. The plots show results of the 5 mg Cu<sup>2+</sup>/L at 300 mL/min, without Ni<sup>2+</sup>, for comparison to flow through experiments when Ni<sup>2+</sup> was present. Triplicate tests were conducted at each concentration. All competitive flow through experiments were conducted at a constant flow rate of 300 mL/min. Taking into consideration the results of the Ni<sup>2+</sup> batch and flow through experiments, the tests were run to determine the effect of the presence of the Ni<sup>2+</sup> on Cu<sup>2+</sup> removal.

The results indicate each charred porous polymer responded differently to the presence of a competing cation. Supelcarb™ responded with equal or greater number of bed volumes to breakthrough, while Carboxen-1011™ responded with all shorter number of bed volumes to breakthrough.

## **4.2 Discussion**

### **4.2.1 Cu<sup>2+</sup> Adsorbing on to Supelcarb<sup>TM</sup> and Carboxen-1011<sup>TM</sup> in the Batch Experiments**

The batch adsorption isotherm for Cu<sup>2+</sup> adsorbing onto Supelcarb<sup>TM</sup> and Carboxen-1011<sup>TM</sup> show an S<sub>MAX</sub> of 10 and 12 mg/g respectively, *Figure 4-1* and *Figure 4-2*. Other commercially available sorbents such as peat and bone char have demonstrated a S<sub>MAX</sub> of 14 mg/g and 100 mg/g, respectively, for the removal of Cu<sup>2+</sup> (Allen, 1996). Allen (1996) did not report the ionic strength used in their experiments. Our tests were performed at relatively high ionic strengths, which could account for the differences reported by Allen (1996). In batch tests, increased ionic strength has been shown to reduce metal adsorption ([Error! Not a valid link.](#)).

Wilczak et al. (1993) showed that it takes copper longer than 10 minutes to reach final equilibrium. Copper has demonstrated biphasic sorption, where copper is removed quickly in about 2.5 days and a slower approach to equilibrium in about 30 days using powdered activated carbon (Wilczak et al. 1993). Tiwari et al. (1998) reports reaching equilibrium sorption with copper in as short as 360 minutes using activated carbon. We only allowed copper to equilibrate for 10 minutes to measure the rapid sorption phase of copper in order to get a feel for the maximum sorption that we could expect during the flow through experiments.

Copper concentrations of less than 10 mg Cu<sup>2+</sup>/L were totally removed in the equilibration time of 10 minutes, *Figure 4-1* and *Figure 4-2*. This result agrees with the

findings of Ong and Swanson (1966) who showed 98% removal of dilute copper concentrations with peat. The  $K_f$  for copper was  $1.92 (L/g)^{1/n}$  with  $n = 0.58$ . Sag et al. (1995) reported a  $K_f$  value of  $3.19 (L/g)^{1/n}$  with  $n = 0.42$  in his research of copper removal with a bioadsorbent. Sag did not have a background electrolyte present and used doubly distilled water as his solvent. His contact time was one hour.

#### **4.2.2 Ni<sup>2+</sup> Adsorbing on to Supelcarb and Carboxen**

In the nickel batch test with Supelcarb<sup>TM</sup> and Carboxen-1011<sup>TM</sup>, *Figure 4-8* and *Figure 4-9*, shows a  $S_{MAX}$  of 0.13 and 1.8 mg/g for Ni<sup>2+</sup> respectively compared to powdered activated carbon with a  $S_{MAX}$  of 1.3 mg/g (Reed *et al.*, 1992). Reed et al. (1992) used an ionic strength of 10 mM of NaNO<sub>3</sub>. Our ionic strength was 100mM of NaCl; which may account for the discrepancy in the Supelcarb<sup>TM</sup> results. The Carboxen-1011<sup>TM</sup> results are very similar to Reed's results indicating that some other factor besides ionic strength caused Supelcarb<sup>TM</sup> to have a smaller adsorption capacity for Ni<sup>2+</sup>.

The one order of magnitude difference between Supelcarb<sup>TM</sup> and Carboxen-1011<sup>TM</sup> adsorption of Ni<sup>2+</sup> could be explained by examining the differences in shape of two porous polymers pores. Supelcarb<sup>TM</sup> has dead end pores while Carboxen-1011<sup>TM</sup> has "hour-glass" shaped pores. The "hour glass" shaped pores are very efficient at removing water molecules that set up around the metal cation (Betz, 1998). The pore diameter decreases as the Ni<sup>2+</sup> is drawn further into the through put pore. The metal cation is de-watered as van der Waals forces draw the molecule into the Carboxen-1011<sup>TM</sup> adsorbent

(Betz, 1998). When a Ni<sup>2+</sup> cation lands in the dead end pore of Supelcarb<sup>TM</sup> the cation is not de-watered and is more easily flushed out of the pore.

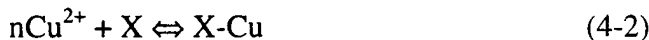
#### **4.2.3 Minteq Chemical Speciation Model of Batch Tests**

Minteq is a geochemical equilibrium model with the ability to model dilute aqueous systems. The model computes equilibrium states among dissolved, adsorbed, solid, and gas phase systems in a natural setting (Allison et al., 1990). This model was applied to the batch data for both Supelcarb<sup>TM</sup> and Carboxen-1011<sup>TM</sup>. The objective of the Minteq model application was to gather chemical speciation and solid phase data from the model results and predict results of a Cu<sup>2+</sup>/Ni<sup>2+</sup> bisolute batch experiment.

The reaction used to describe the adsorption of Cu<sup>2+</sup> or any other metal cation can be described by the following stoichiometric reaction:



where X is the adsorbent and X-Cu describes the new compound created by the adsorption of Cu<sup>2+</sup> onto X. Since, the Freundlich adsorption model is being applied the adsorption mass action equation is as follows:



The mass action coefficient, n, is same coefficient that was developed in section 4.1.1.1.

*Figure 4-1 and Figure 4-2* define K<sub>f</sub> and n for the Cu<sup>2+</sup> batch tests. These coefficients were input into the Minteq model. Minteq rearranges equation (4-2) to model the adsorption reaction using the following equation.

$$K_f = \frac{[X - Cu]}{[Cu^{2+}]^r [X]} \quad (4-3)$$

The amount sorbed is given by

$$[Cu^{2+}]^r K_f = [X - Cu] \quad (4-4)$$

The Minteq model results are plotted with the Freundlich model and observed data points for both Supelcarb<sup>TM</sup> and Carboxen-1011<sup>TM</sup> see *Figure 4-22* and *Figure 4-23* respectively. These figures show that Minteq mirrored the Freundlich model well. This was to be expected since the Minteq model uses the same empirical values that were determined from the Freundlich model which was arrived at from experimental data.

The results of the Ni<sup>2+</sup> adsorption tests were used to derive the Freundlich adsorption isotherm coefficients and these parameters were input into Minteq as described in section 4.1.1.2. The plot of the Minteq results, the Freundlich Model and observed data can be found in *Figure 4-16* and *Figure 4-17*. The model results indicate that the Freundlich adsorption coefficient ,K<sub>f</sub>, even though it is weak, is still strong enough to cause the Ni<sup>2+</sup> to bond with the adsorbent instead of forming Ni(OH)<sub>2</sub>.

After modeling each of the single solute system, the Freundlich adsorption coefficients for copper and nickel were input into Minteq to model a bisolute batch reaction. The objective was to simultaneously model the adsorption of copper and nickel onto each adsorbent, Supelcarb<sup>TM</sup> and Carboxen-1011<sup>TM</sup>. Unfortunately, the Freundlich adsorption model assumes that the adsorbent has an infinite amount of adsorption sites.

This assumption caused the result of the model runs to be identical to each of the batch experiments, *Figure 4-81* and *Figure 4-19*. In essence the model super imposed each of the single solute batch model results onto each other. This result was to be expected if the adsorbents had infinite adsorption sites. However, this is not the result that would have occurred if a bisolute batch experiment was actually conducted. In reality there is a finite amount of adsorption sites and the presence of competing metal cations should reduce the overall adsorption of each metal (Reed and Nonavinakere, 1992).

#### **4.2.4 Feasibility Analysis on the Use of Microporous Treatment of Metal Contaminated Storm Water by Charred Microporous Polymers**

The Norfolk Naval Shipyard is the main homeport for the Atlantic Fleet. The shipyard operates four graving docks. Dry dock 8 is the largest of the four and is capable of berthing the USS Lincoln the Navy's largest ship. This dry dock encompasses an area of 1,125 feet by 188 feet (Key et al. 1995). Liquids enter the dry dock from several sources like ship's cooling water, rainwater, and hydrostatic leaking. These liquids come in contact with exposed metal, metal containing paint particles, and anti-foulent solvents containing copper. This exposure results in the liquid being contaminated with heavy metals prior to being discharged via the dry docks drainage system.

The Norfolk Naval Shipyard is particularly concerned with copper contamination in the effluent of Dry dock 8. The shipyard has received notices of violation from the Virginia Department of Environmental Quality for discharges at Dry dock 8 containing

an average concentration of 0.438 mg Cu<sup>2+</sup>/L and violating the permitted discharge amount of 0.335 mg Cu<sup>2+</sup>/L (Host 1996).

The charred microporous polymers that have been experimentally evaluated will be analyzed to estimate the filter service time that might be expected if the charred microporous polymers were employed as part of an in-line storm water treatment process at Dry Dock 8. To make this analysis storm data was collected to determine design storm water flows for a six hour 1, 2, 5, and 10 year storm events shown in (Roberson et al. 1988). The filter will be sized to fit inside the outlet pipe of a Stormceptor® I oil/water separator (*Figure 2-3*) which has a design flow of 0.4 million gallons per day (MGD).

In order to estimate the filter service time in a field environment using results gained from laboratory experiments some assumptions must be made. The number of bed volumes to break through are proportional to the ratio of effluent concentration to the influent concentration and flow rate. A linear relationship between the influent concentration and the number of bed volumes to break through must exist. Finally, no other competitive or synergistic effects can be present in the storm water.

Next the number of bed volumes to break through points for both Supelcarb<sup>TM</sup> and Carboxen-1011<sup>TM</sup> are plotted versus Cu<sup>2+</sup> influent concentration. A trend line has been plotted through these points shown in *Figure 4-20* and *Figure 4-21* for Supelcarb<sup>TM</sup> and Carboxen-1011<sup>TM</sup> respectively. The equation of the line for *Figure 4-20* and *Figure 4-21* is shown in equation (4-5) and equation (4-6) respectively.

$$[\text{Cu}^{2+}] = -0.0979 \text{ BV} + 14.55 \quad (4-5)$$

$$[\text{Cu}^{2+}] = -0.049 \text{ BV} + 12.3 \quad (4-6)$$

Using equation (4-5) and equation (4-6) bed volumes, BV is solved for by making the influent copper concentration,  $[\text{Cu}^{2+}]$  equal  $0.438 \text{ mg Cu}^{2+}/\text{L}$  the average copper concentration in storm water at Dry dock 8. Consequently, the number of bed volumes to break through is 144 and 242 for Supelcarb<sup>TM</sup> and Carboxen-1011<sup>TM</sup>. Recall that breakthrough was defined as 10% of the influent concentration for the flow through experiments as shown in *Figure 4-5* and *Figure 4-7*. This scenario requires a breakthrough definition of  $(0.335 \text{ mg Cu}^{2+}/\text{L})/(0.438 \text{ mg Cu}^{2+}/\text{L}) = 76\%$ . To estimate a 76% break through the  $2.5 \text{ mg Cu}^{2+}/\text{L}$  curve shown *Figure 4-5* and *Figure 4-7* must be extended linearly to 76% break through. This results in 950 bed volumes to break through at 76% an increase of a factor of 7.6 from 125 bed volumes to breakthrough at 10%. A factor of 7, to be conservative, will be used to convert the 10% bed volumes to break through to the number of bed volumes at break through of 76%. Multiplying this factor times the 10% number of bed volumes to break through results in 1,008 and 1,694 bed volumes to 76% of the influent concentration for Supelcarb<sup>TM</sup> and Carboxen-1011<sup>TM</sup>. The filter service time is the product of the number of bed volumes to break through at 76% and the empty bed contact time (EBCT) of the filter. The filter service times are tabulated in *Table 4-3* for both Supelcarb<sup>TM</sup> and Carboxen-1011<sup>TM</sup>.

The estimates of filter service time show that the charred microporous polymer filter would last 3.5 hours and 6 hours for Supelcarb<sup>TM</sup> and Carboxen-1011<sup>TM</sup> respectively during a 1 year six hour storm event. This means that Carboxen-1011<sup>TM</sup>

*Table 4-3: Analysis of charred microporous polymers as an in-line storm water treatment system.*

|                | Storm Frequency (yr)<br>6 Hour Duration |      | Bed Volume to Break Through | Filter Service Time (min) |
|----------------|---|------|-----------------------------|---------------------------|
| Supelcarb™     | 1                                       | 0.21 | 1,008                       | 212                       |
|                | 2                                       | 0.17 | 1,008                       | 171                       |
|                | 5                                       | 0.11 | 1,008                       | 111                       |
|                | 10                                      | 0.10 | 1,008                       | 101                       |
| Carboxen-1011™ | 1                                       | 0.21 | 1,694                       | 356                       |
|                | 2                                       | 0.17 | 1,694                       | 288                       |
|                | 5                                       | 0.11 | 1,694                       | 186                       |
|                | 10                                      | 0.1  | 1,694                       | 169                       |

could successfully treat a 1 year, 6 hour storm event, but stronger storms would require filter replacement during the storm event.

This design could be improved upon by selecting an inline storm treatment process that could house a larger filter cartridge. This would increase the EBCT and would significantly improve the filter service time for both carbons. The filters could be placed in series effectively increasing the depth of the filter cartridge resulting in an increase in service filter time. Finally, a better adsorber could be selected that would be more efficient at removing copper ions.

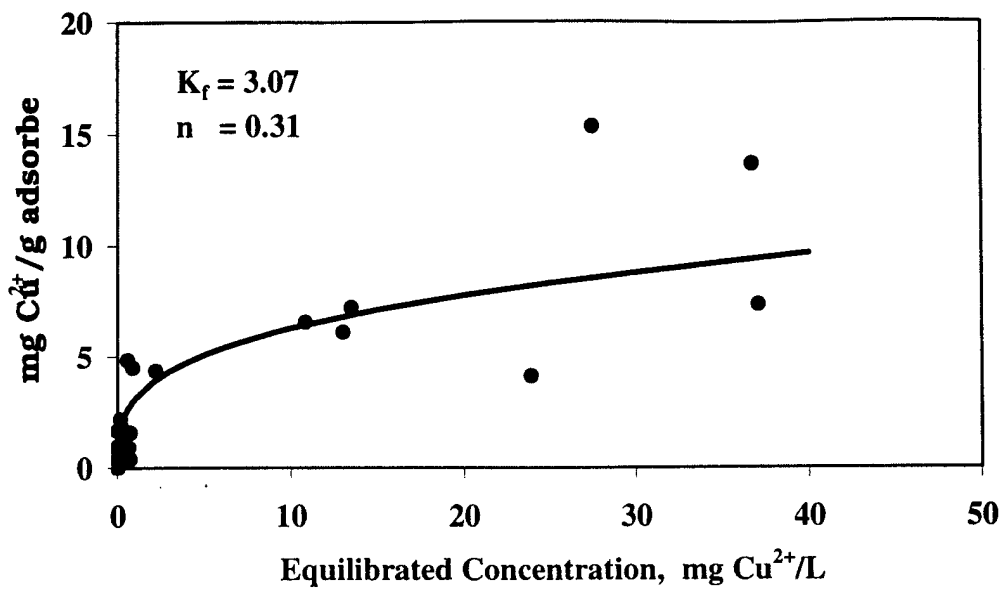


Figure 4-1: Copper adsorption isotherm obtained with Supelcarb™ in the batch experiments.

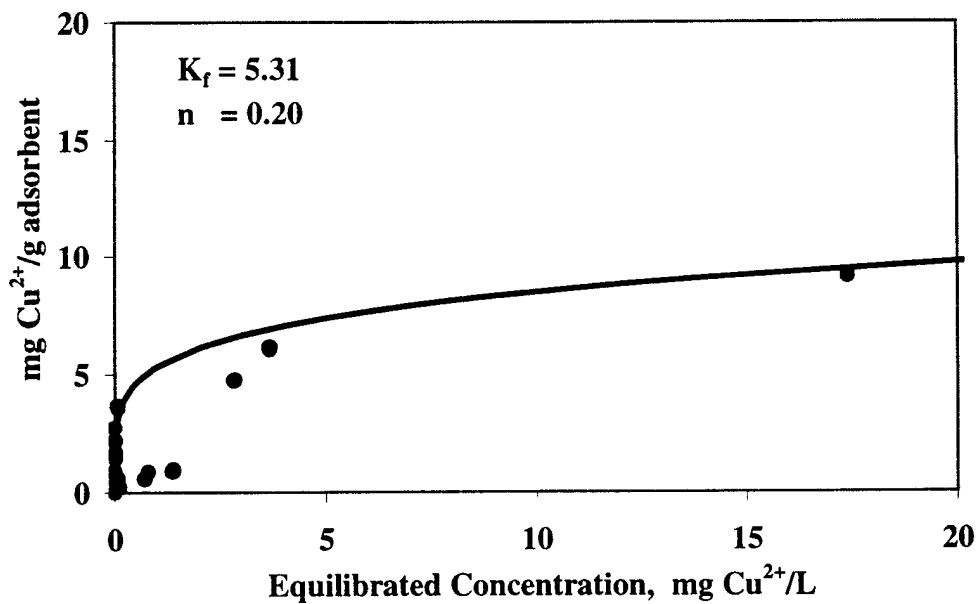


Figure 4-2: Copper adsorption isotherm obtained with Carboxen-1011™ in the batch experiments.

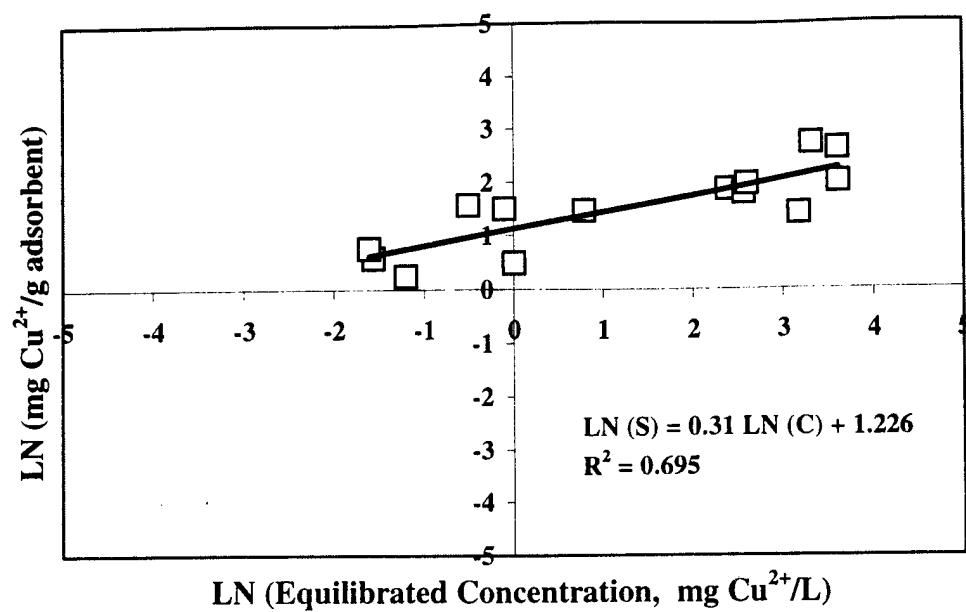


Figure 4-3: Freundlich adsorption isotherm obtained with Supelcarb<sup>TM</sup> in the batch experiments.

---

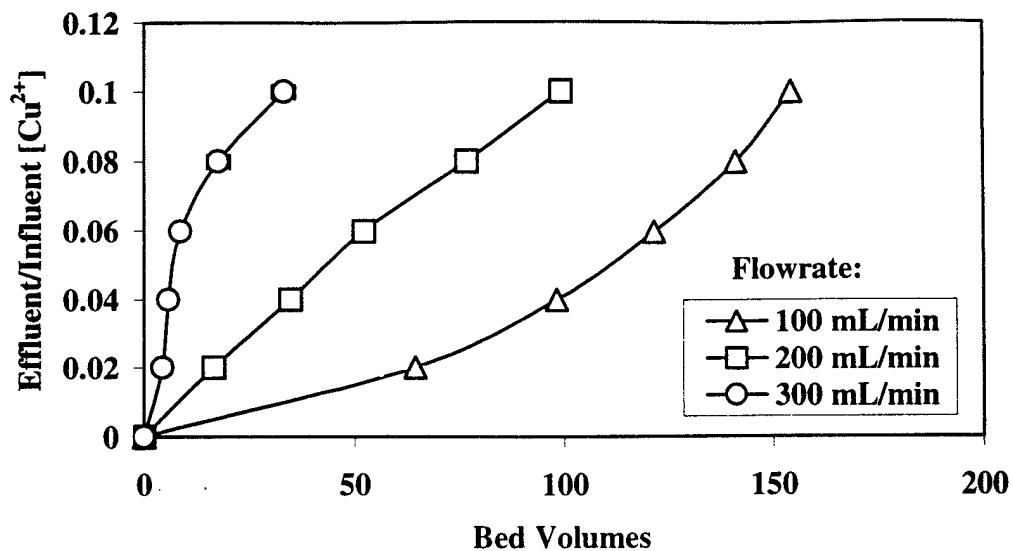


Figure 4-4: Copper breakthrough curves obtained with Supelcarb<sup>TM</sup> and a constant influent concentration of 5 mg Cu<sup>2+</sup>/L in the flow through experiments. Error bars represent a standard deviation about a triplicate mean.

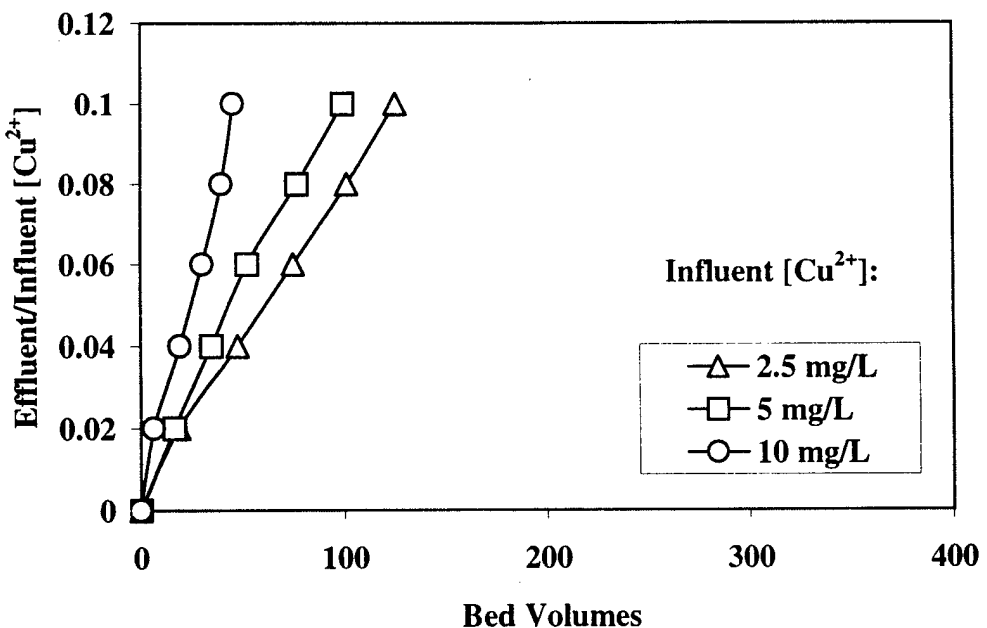


Figure 4-5: Copper breakthrough curves obtained with Supelcarb<sup>TM</sup> and a constant flow rate of 200 mL/min in the flow through experiments. Error bars represent a standard deviation about a triplicate mean (10 mg/L error bar no larger than symbol size).

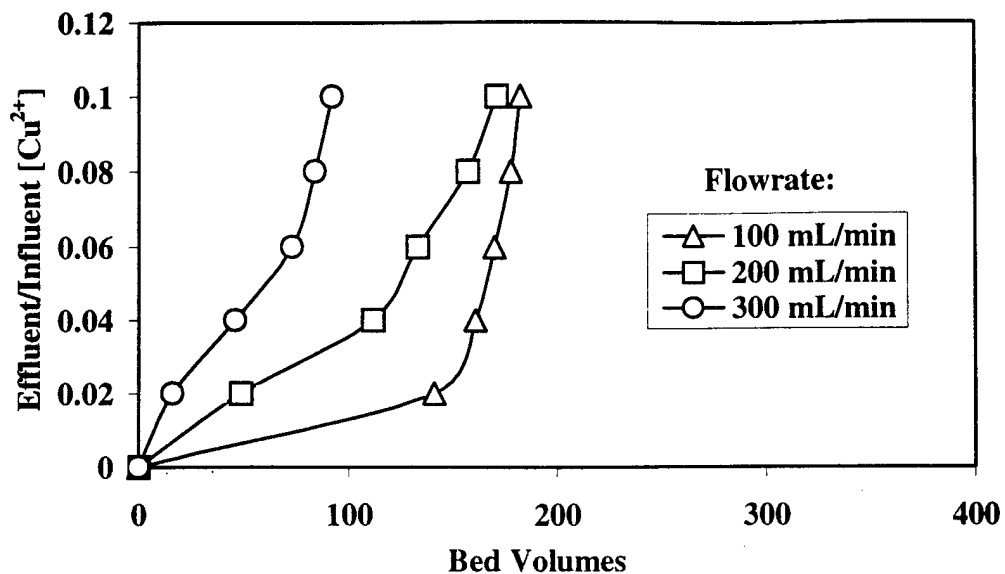


Figure 4-6: Copper breakthrough curves obtained with Carboxen-1011<sup>TM</sup> and a constant influent concentration of 5 mg Cu<sup>2+</sup>/L in the flow through experiments. Error bars represent a standard deviation about a triplicate mean.

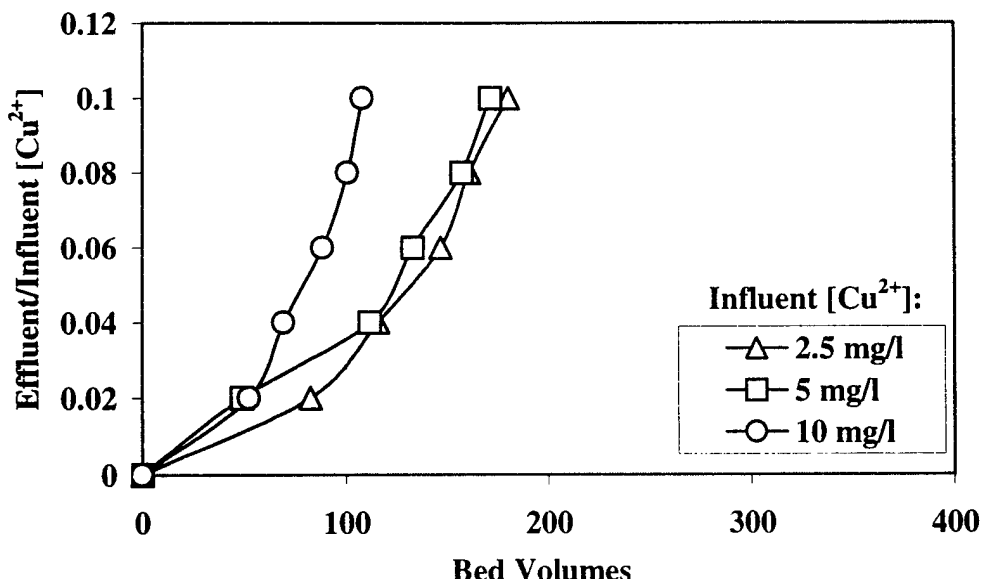


Figure 4-7: Copper breakthrough curves obtained with Carboxen-1011<sup>TM</sup> and a constant flow rate of 200 mL/min in the flow through experiments. Error bars represent a standard deviation about a triplicate mean (10 mg/L error bar no larger than symbol size).

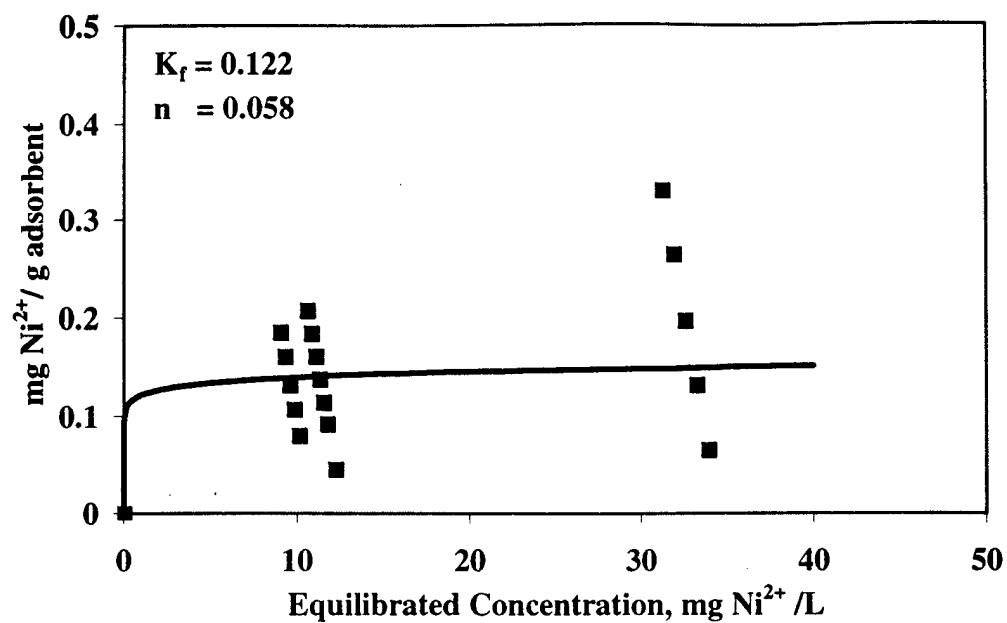


Figure 4-8: Nickel adsorption isotherm obtained with Supelcarb<sup>TM</sup> in the batch experiments.

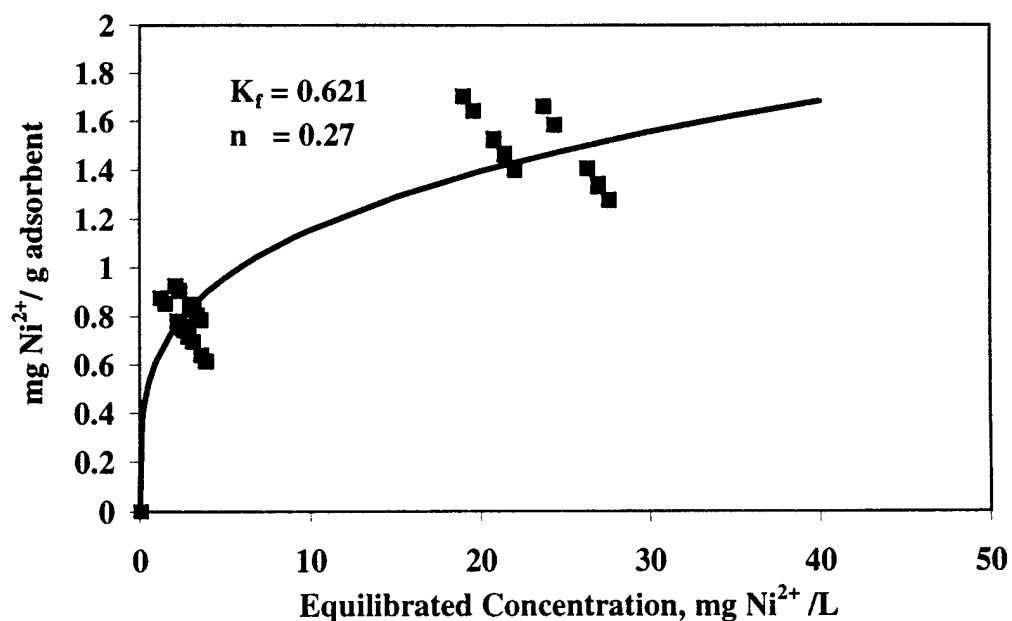


Figure 4-9: Nickel adsorption isotherm obtained with Carboxen-1011<sup>TM</sup> in the batch experiments.

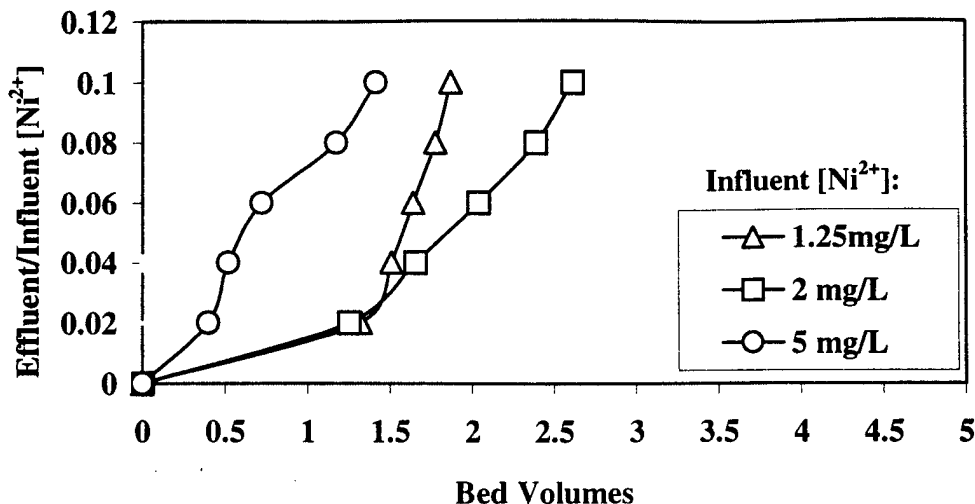


Figure 4-10: Nickel breakthrough curves obtained with Supelcarb™ and a constant flow rate of 200 mL/min in the flow through experiments. Error bars represent a standard deviation about a triplicate mean.

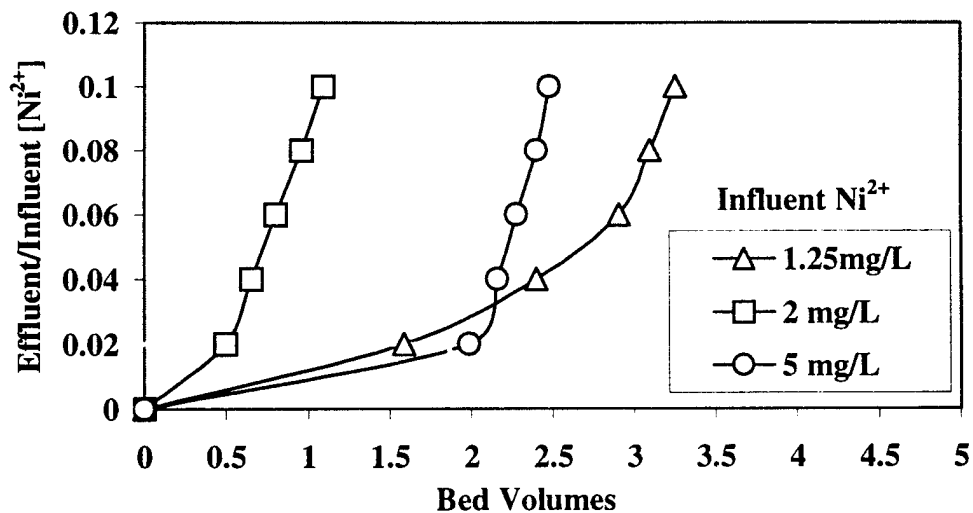


Figure 4-11: Nickel breakthrough curves obtained with Carboxen-1011™ and a constant flow rate of 200 mL/min in the flow through experiments. Error bars represent a standard deviation about a triplicate mean.

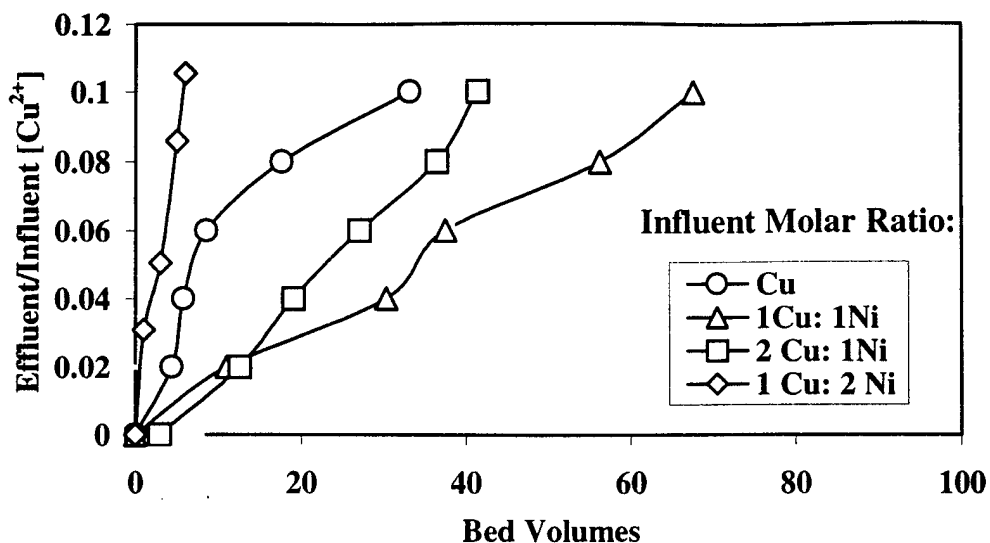


Figure 4-12: Copper breakthrough in a  $\text{Cu}^{2+}/\text{Ni}^{2+}$  bisolute system. Curves obtained with Supelcarb™ and a constant flow rate of 300 mL/min in the flow through experiments. Error bars represent a standard deviation about a triplicate mean.

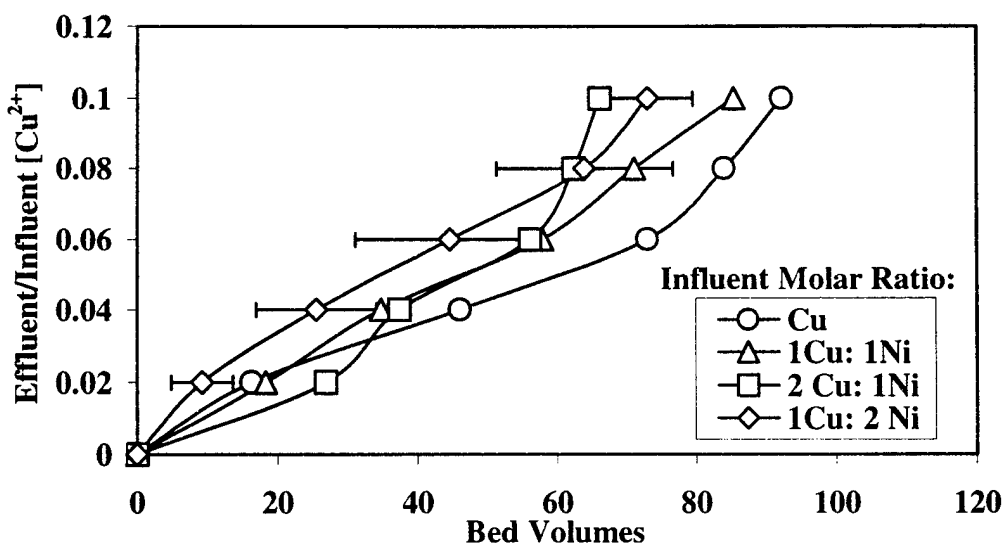


Figure 4-13: Copper breakthrough in a  $\text{Cu}^{2+}/\text{Ni}^{2+}$  bisolute system. Curves obtained with Carboxen-1011™ and a constant flow rate of 300 mL/min in the flow through experiments. Error bars represent a standard deviation about a triplicate mean.

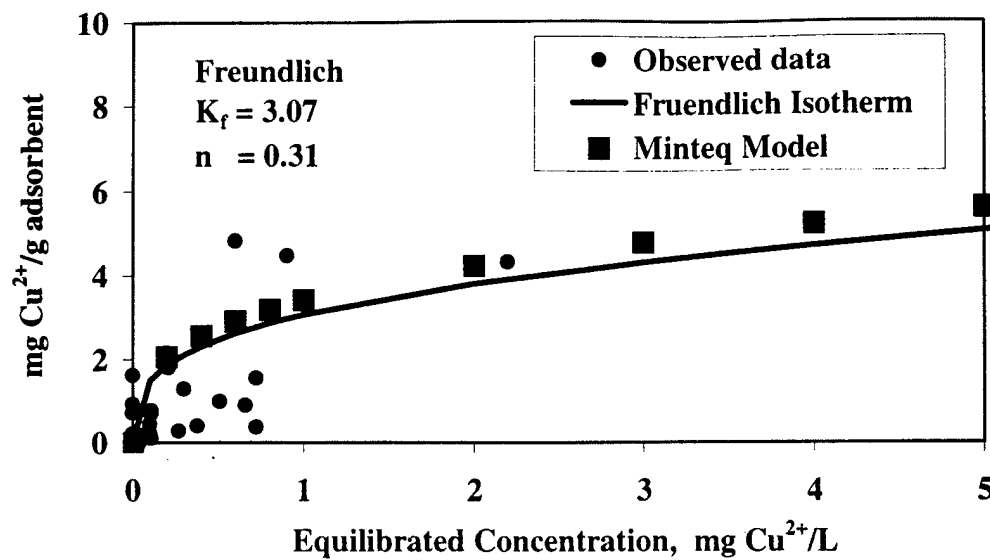


Figure 4-14: Copper adsorption isotherm obtained with Supelcarb<sup>TM</sup>. Minteq model results plotted as dark square.

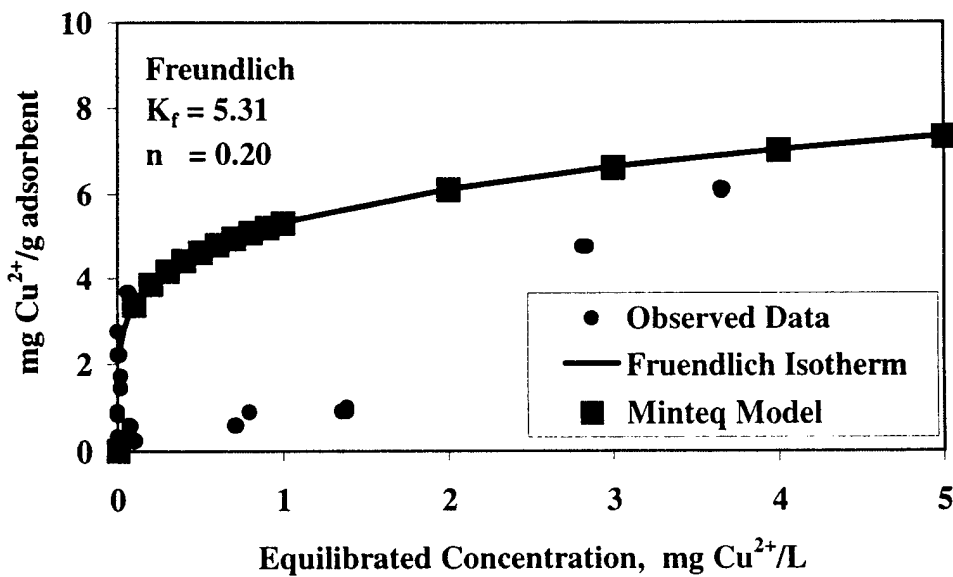


Figure 4-15: Copper adsorption isotherm obtained with Carboxen-1011<sup>TM</sup>. Minteq model results plotted as dark square.

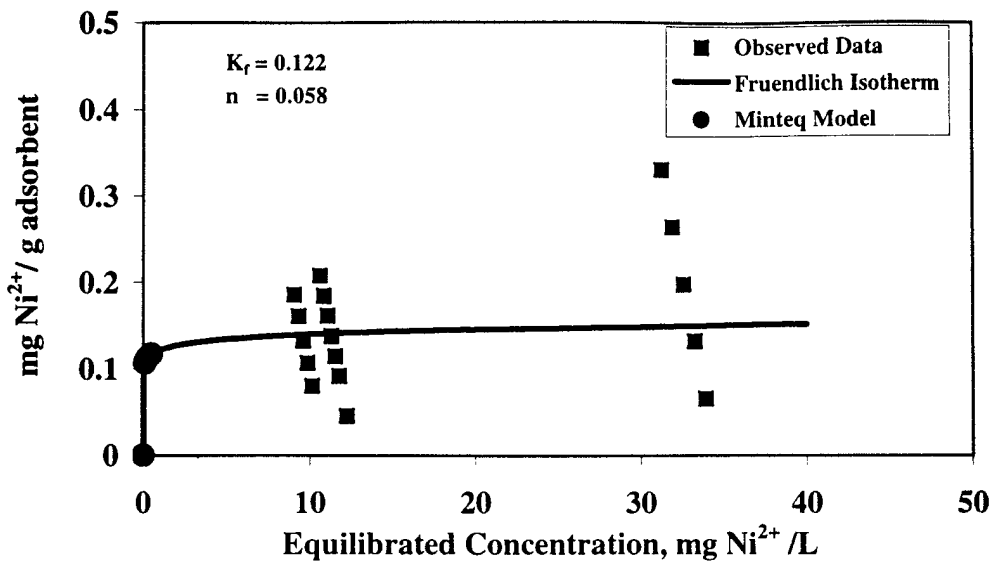


Figure 4-16: Nickel adsorption isotherm obtained with Supelcarb™ in the batch experiments with Minteq model results.

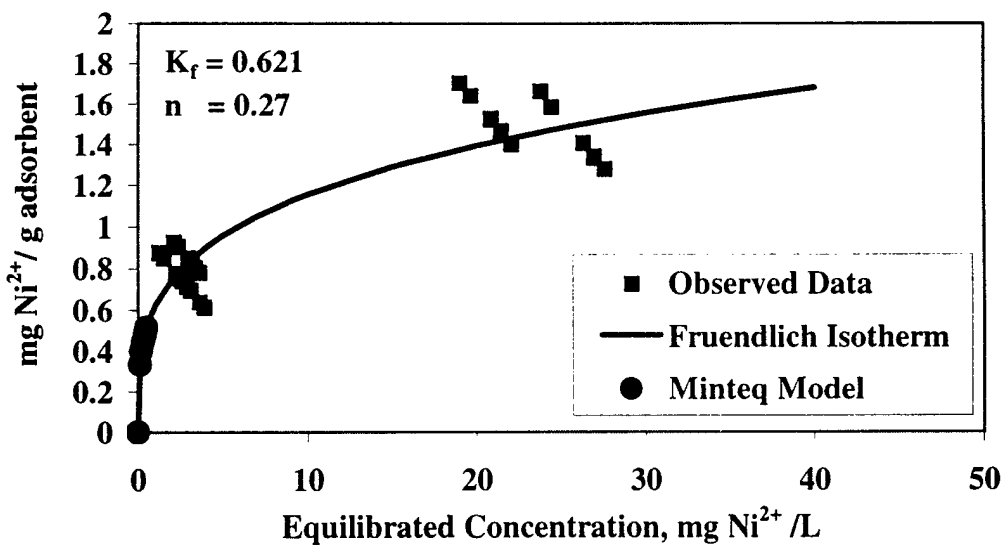


Figure 4-17: Nickel adsorption isotherm obtained with Carboxen-1011™ in the batch experiments with Minteq model results.

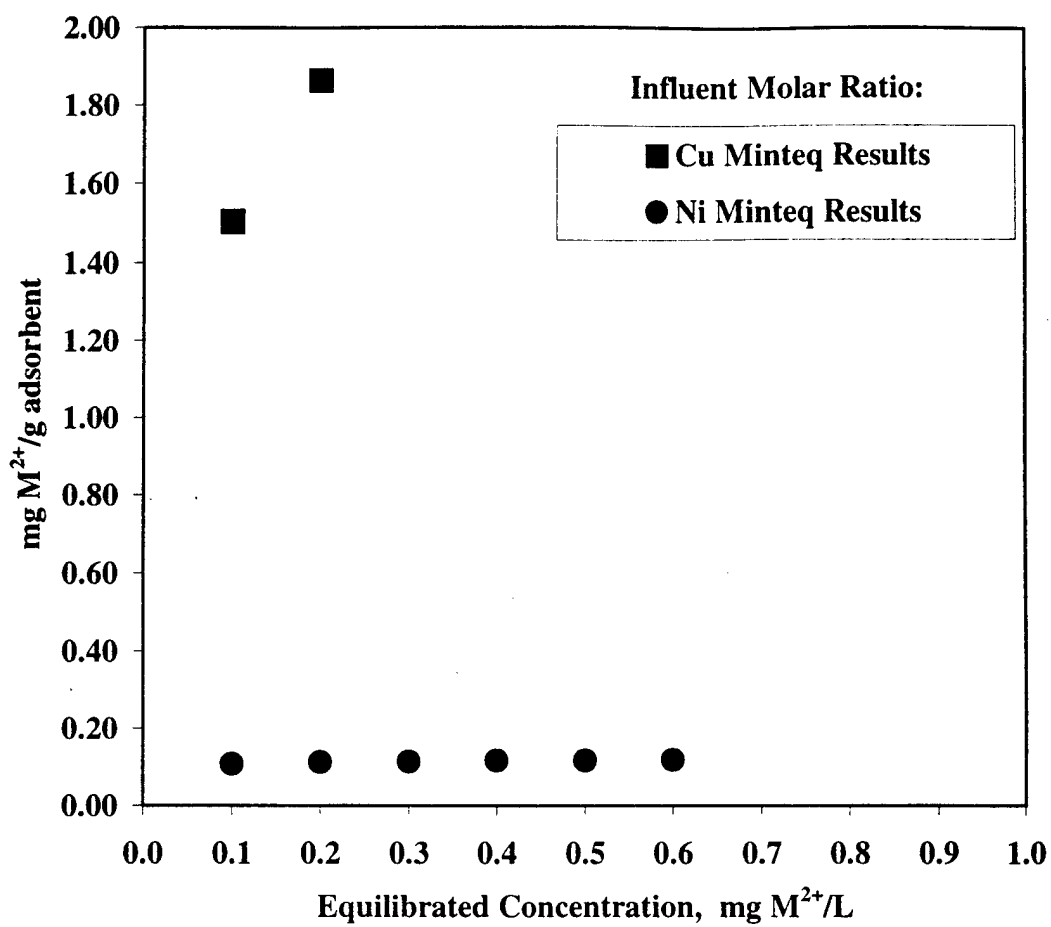


Figure 4-18: Minteq model of a combined  $\text{Ni}^{2+}$  and  $\text{Cu}^{2+}$  batch adsorption experiment with Supelcarb<sup>TM</sup>. Minteq simply super imposed the adsorption isotherms for each metal. This result is caused by Minteq's assumption of infinite adsorption sites on the charred porous polymers.

---

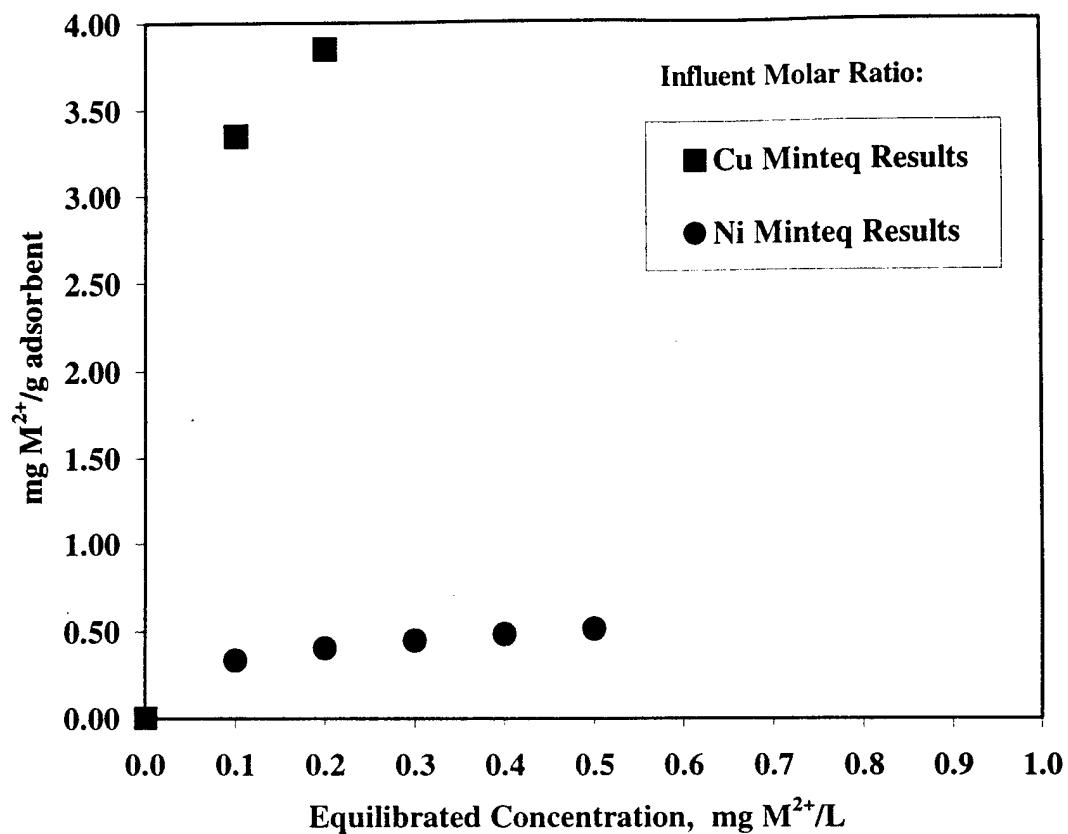


Figure 4-19: Minteq model of a combined  $\text{Ni}^{2+}$  and  $\text{Cu}^{2+}$  batch adsorption experiment with Carboxen-1011<sup>TM</sup>. Minteq simply super-positioned the adsorption isotherms for each metal. This result is caused by Minteq's assumption of infinite adsorption sites on the charred porous polymers.

---

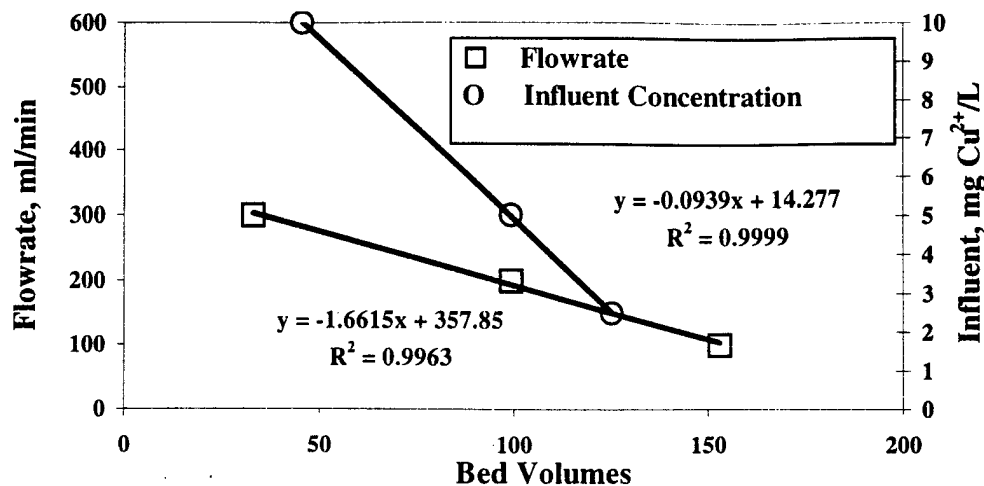


Figure 4-20: Graph demonstrating the linear relationship between flow rate, influent  $\text{Cu}^{+2}$  and bed volumes to filter breakthrough using Supelcarb™. This analysis should be used for metal filter design.

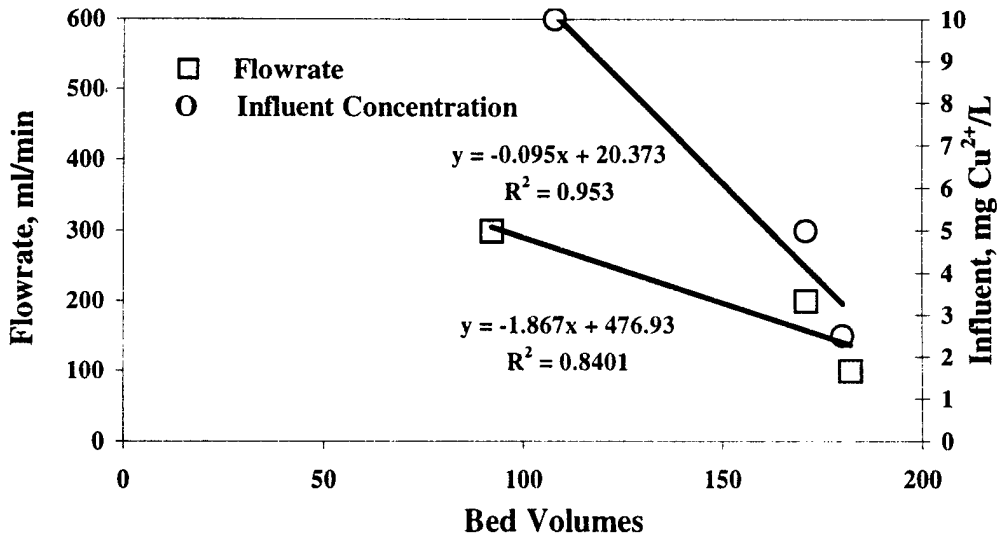


Figure 4-21: Graph demonstrating the linear relationship between flow rate, influent  $\text{Cu}^{+2}$  and bed volumes to filter breakthrough using Carboxen-1011™. This analysis should be used for metal filter design.

## Chapter 5

### CONCLUSIONS AND RECOMMENDATIONS

This study evaluated the feasibility of using charred microporous polymers as adsorbents to remove  $\text{Cu}^{2+}$  and  $\text{Ni}^{2+}$  from a saline synthetic storm water. Results indicated that  $\text{Cu}^{2+}$  was effectively removed but not  $\text{Ni}^{2+}$ . There are storm water collection systems commercially available that could be readily equipped with an in-line porous adsorber to remove dissolved contaminants. A scenario was conducted to estimate the filter service time when Supelcarb<sup>TM</sup> and Carboxen-1011<sup>TM</sup> are placed with in an existing storm water treatment system. Results of the scenario indicates that the adsorbents tested had 6 hours or less filter service time which decreased with increasing storm intensity. However, this pollution prevention technology is feasible, but will require additional research for adsorbent selection and process performance prediction. The following conclusions can be drawn from this study:

#### 5.1 Conclusions

- ☒ Copper was more effectively removed in the batch experiments than  $\text{Ni}^{2+}$  with both Supelcarb<sup>TM</sup> and Carboxen-1011<sup>TM</sup> as adsorbents.
- ☒ Copper concentrations were totally removed in the batch experiments for copper concentrations of less than 10 mg  $\text{Cu}^{2+}/\text{L}$ .

- ☒ Carboxen-1011<sup>TM</sup> and Supelcarb<sup>TM</sup> are identical adsorbents except Carboxen-1011<sup>TM</sup> has throughput pores and Supelcarb<sup>TM</sup> has dead end pores. Ni<sup>2+</sup> showed a greater affinity for Carboxen-1011<sup>TM</sup> with the throughput pores.
- ☒ In the estimation of filter service times during actual storm events for the Norfolk Naval Shipyard neither of the adsorbers preformed at a level that would be useful in industry.
- ☒ More research is required to select a more efficient adsorber for the removal of metals.
- ☒ Treatment of metal contaminated storm water is feasible using an in-line adsorber.

## **5.2 Recommendations**

- ☒ A longer contact time should be used in the batch tests to allow the metal solution to come into equilibrium with the adsorbent.
- ☒ The batch test should be used screen metals before the flow through test. If a metal cation does not adsorb well in the batch experiments than it will not adsorb well in the flow through tests.
- ☒ Competing metal cation adsorptions experiments should only be conducted with metal cations that adsorb well in the batch tests.
- ☒ Future metal adsorption tests should include studying the effects of varying ionic strength.
- ☒ Acid wash the charred microporous polymer prior to use.

- ☒ Operate column flow through experiments until the influent concentration equals the effluent concentration or local equilibrium is achieved.
- ☒ Use lower contaminant concentration ranges to more accurately reflect contaminated storm water found in industry.
- ☒ Establish pH controls for the effluent flow rather than the influent flow.

## BIBLIOGRAPHY

Allen, S. J.(1996). Types of Adsorbent Materials. In Adsorbents McKay (Ed.)(pp. 59-97). New York: CRC Press.

Allison, Jerry D., David S. Brown, and Kevin J. Novo-Gradac. (1990). MinteqA2/ProdefA2, A Geochemical Assessment Model for Environmental Systems: Version 3.0 User's Manual. Envionmental Research Laboratory, Office of Research and Development, U.S. Environmental Protection Agency. Athens, GA.

American Public Health Association, American Water Works Association, and Water Pollution Control Federation. (1995). Standard Methods for Examination of Water and Wastewater. 16<sup>th</sup> ed. Edited by Mary Ann H. Franson. Washington, D.C.: American Public Health Association.

Anderson, B. C., W. E. Watt, J. Marsalek, and A.A. Crowder. (1996). Integrated Urban Stormwater Quality Management: field Investigations at a Best Management Facility. Canadian Water Resources Journal. 21 (2), 165-182.

Badri, M. and Karen A. Crouse. (1989). Changes in Surface Potential of Activated Carbon Due to Adsorption of Ions. Pertanika. 12 (1), 66-70.

Betz, Bill. Chief Research Chemist Supelco Inc., Manufacturer of Supelcarb and Carboxen. Personal Interview. March 1998.

Brown, P., O. Flynn, G. McKay, S.J. Allen. (1992). The evaluation of various adsorbents for the removal of heavy metals from waste waters. International Chemical Engineering Conference. 152-154.

Chang, Chung and Young Ku. (1995). The Adsorption and Desorption Characteristics of EDTA- Chelated Copper Ion by Activated Carbon. Separation Science and Technology. 30(6), 899-915.

Duggan, Orna and Stephen J. Allen. (1997). Study of the Physical and Chemical Characteristics of a Rang of Chemically Treated, Lignite Based Carbons. Water Science Technology. 35 (7), 21-27.

Dunn, Chris, S. Brown, G.K. Young, S. Stein, and M.P. Mistichelli. (1995). Current Water Quality Best Management Practices Design Guidance. Transportation Research Record No. 1483. Washington D.C.:National Academy Press. 80-88.

Ellwood and William D. Burgos. To be published. Regulatory Methods used in writing NPDES Permits for the Shipbuilding and Repair Industry. Journal of Environmental Management.

EPA. (1983b). Results of the Nationwide Urban Runoff Program: Volume 1-Final Report. Water Planning Division WH-554. Washington, D.C.

EPA. (1991). Technical Support Document of Water Quality-based Toxics Control. EPA/505/2-90-001. Washington, D.C.

EPA. (1992). Impacts of Storm Water Discharges a National Profile. EPA 841-R-92-001, EPA Office of Water, Washington, D.C.

EPA. (1993). Water Pollution Control, NPDES General Permits and Fact Sheets; Storm Water Discharges from Industrial Activities; Proposed Rule. 58 Federal Register 222.

Faust, Samuel D. and Osman M. Aly. (1987). Adsorption Processes for Water Treatment. Boston: Butterworths Publishers. (

Feng, X, G. E. Fryxell, L. Q. Wang, Ay Kim, J. Liu, K. M. Kemner. (1997). Functionalized Monolayers on Ordered Mesoporous Supports. Science. 276:923-925.

Fifield, F. W. and P. J. Haines, ed. (1995). Environmental Analytical Chemistry. London: Blackie Academic & Professional.

Host, Phillip M. (1996). Drydock Water Pollution control Efforts at Norfolk Naval Shipyard. Naval Engineer's Journal. 57-64.

Jenkins, G.M. and K. Kawamura. (1976). Polymeric Carbons- Carbon Fibre, Glass and Char. New York: Cambridge University Press.

Key, G. S., P. J. Earley, and M. Caballero. (1995). An Integrated Marine Environmental Compliance Program for Naval Shipyards: Phase I Report. Prepared for NAVSEA 07E, Shore Activity Environment Office and OSH Office.

Line, Daniel E., Jon A. Arnold, Gregory D. Jennings, and Jy Wu. (1996). Water Quality of Storm water Runoff from Ten Industrial Sites. Water Resources Bulletin. 32 (4), 807-816.

Matsumoto, Mark R., A. Scott Weber, James H. Kyles. (1989). Use of Metal Adsorbing Compounds (MAC) to Mitigate Adverse Effects of Heavy Metal in Biological Unit Processes. Chemical Engineering Communications. 86, 1-16

Ong, H. Ling and Vernon E. Swanson. (1966). Adsorption of Copper by Peat, Lignite, and Bituminous Coal. Economic Geology. 61(5), 1214-1231.

Reed, Brian E. and Sujith Kumar Nonavinakere. (1992). Metal Adsorption by Activated Carbon: Effect of Complexing Ligands, Competing Adsorbates, Ionic Strength, and Background Electrolyte. Separation Science and Technology. 27(14), 1985-2000.

Roberson, John A., John J. Cassidy, and M. Hanif Chaudry. (1988). Hydraulic Engineering. Houghton Mifflin Company. Boston.

Sag, Y. and T. Kutsal. (1995). Copper (II) and Nickel (II) Adsorption by Rhizopus arrhizus in Batch Stirred Reactors in Series. The Chemical Engineering Journal. 58, 265-273.

Schwarzenbach, Rene P., Philip M. Gschwend, and Dieter M. Imboden. (1993). Environmental Organic Chemistry. New York: John Wiley and Sons Inc.

Schnoor, Jerald L. (1996). Environmental Modeling Fate and Transport of Pollutants in Water, Air, and Soil. New York: John Wiley and Sons Inc.

Snoeyink, Vernon L. (1990). Adsorption of Organic Compounds. In F. W. Pontius (Ed.), Water Quality and Treatment: A Handbook of Community Water Supplies (4<sup>th</sup> ed.) (pp. 781-875). New York: McGraw-Hill.

Tiwari, D. P., K. Promod, A.K. Mishra, R. P. Singh, and R. P. S. Srivastav. (1989). Removal of Toxic Metals from Electroplating Industries (Effect of pH on Removal by Adsorption). Indian Journal of Environmental Health. 31 (2), 120-124.

Wilczak, Andrzej and Thomas M. Keinath. (1993). Kinetics of Sorption and Desorption of Copper (II) and Lead (II) on Activated Carbon. Water Environment Research. 65(3), 238-244.